



Mechanism of RHOGDI: Regulation and dysregulation of RHO GTPase membrane trafficking

Dissertation

This dissertation is submitted
for the degree of the *Doctor of Philosophy*
to the Faculty of mathematic and natural science
at the Heinrich-Heine-University Düsseldorf

Written and presented by
Mohammad Akbarzadeh
from Torbatheydarieh, Iran

Düsseldorf, December, 2018



RHOGDI Mechanismus: Regulation und Fehlregulation des RHO GTPasen Membrantransports

Inaugural-Dissertation

zur Erlangung des Doktorgrades
Mathematisch-Naturwissenschaftlichen Fakultät
der Heinrich-Heine-Universität Düsseldorf

vorgelegt von

Mohammad Akbarzadeh

aus Torbatheydarieh, Iran

Düsseldorf, Dezember, 2018

aus dem Institut für Biochemie und Molekularbiologie II
der Heinrich-Heine-Universität Düsseldorf

Gedruckt mit der Genehmigung der
Mathematisch-Naturwissenschaftlichen Fakultät der
Heinrich-Heine-Universität Düsseldorf

Referent: Prof. Dr. Reza Ahmadian
Korreferent: Prof. Dr. Georg Groth

Tag der mündlichen Prüfung:, 2019

To the apples, Gholamreza and Fakhri!
and the broken apples, Mr. Khan and Mehri!
and their immortal-smile.

“Ich glaube, man sollte überhaupt nur noch solche Bücher lesen, die einen beißen und stechen. Wenn das Buch, das wir lesen, uns nicht mit einem Faustschlag auf den Schädel weckt, wozu lesen wir dann das Buch? Ein Buch muß die Axt sein für das gefrorene Meer in uns.“

Franz Kafka

Table of content

| | |
|---|----|
| List of abbreviations | 10 |
| Amino acids abbreviation | 12 |
| Summary..... | 13 |
| Zusammenfassung..... | 14 |
| 1. Introduction | 15 |
| 1.1. RHO GTPase activation and function | 15 |
| 1.2. Regulation of RHO GTPases..... | 16 |
| 1.2.1. Guanine nucleotide exchange factor (GEF)..... | 16 |
| 1.2.2. GTPase-activating proteins (GAP) | 17 |
| 1.2.3. RHOGDI: structure and function..... | 17 |
| 1.2.4. RabGDI..... | 19 |
| 1.3. Posttranslational modification | 20 |
| 1.3.1. Prenylation of RHO GTPases..... | 20 |
| 1.3.2. Phosphorylation and acetylation of GDI..... | 21 |
| 1.4. Impact of membrane lipids on RHO signaling..... | 21 |
| Aims | 22 |
| 2. Material and methods..... | 22 |
| 2.1. Constructs..... | 22 |
| 2.2. Softwares and programs | 24 |
| 2.3. Antibodies, media and reagents | 24 |
| 2.4. Baculoviruses and insect cell culture..... | 24 |
| 2.5. Protein purification and nucleotide exchange | 25 |
| 2.6. Mass Spectrometry | 25 |
| 2.7. Liposome preparation..... | 26 |
| Calculation of RAC1 molecule per liposome..... | 26 |
| 2.8. Kinetics of the protein-protein interaction..... | 27 |
| 2.8.1. Stopped flow measurement..... | 27 |
| 2.8.2. Fluorescence polarization..... | 28 |
| 2.9. Liposome reconstitution of RHO protein displacement by GDI | 28 |
| 2.9.1. Sedimentation assay..... | 28 |
| 2.9.2. Flotation assay | 29 |

| | | |
|---------|--|----|
| 2.10. | Surface plasmon resonance analysis..... | 29 |
| 2.10.1. | GDI direct interaction with RHO | 29 |
| 2.10.2. | RHO interaction with liposome..... | 30 |
| 2.11. | GST-GDI pull down assay | 30 |
| 3. | Results..... | 30 |
| 3.1. | Chapter I: GDI mechanism of function..... | 30 |
| 3.1.1. | Kinetics of the GDI/RHO protein interactions..... | 30 |
| 3.1.2. | Liposomal reconstitution of RHO and GDI interaction..... | 36 |
| 3.1.3. | Kinetic analysis of RHO membrane cycling | 44 |
| 3.2. | Chapter II: GDI in disease | 50 |
| 3.2.1. | CDC42 new mutant (R186C) found in patients showed GDI binding deficiency ... | 50 |
| 3.2.2. | New chemical compound inhibits GDI interaction with RHO GTPase | 53 |
| 4. | Discussion..... | 58 |
| | Acknowledgements | 64 |
| 5. | References..... | 65 |
| | Erklärung zur Dissertation | 71 |

List of figures

| | |
|---|----|
| Figure 1 General activation cycle of RHO GTPases. There are three classes of regulators controlling RHO GTPase activation cycle. | 19 |
| Figure 2 Interaction matrix is launched to demonstrate interaction residues in all available structures. | 32 |
| Figure 3 Coomassie dye gel of purified RHO proteins from <i>E. coli</i> expression system..... | 33 |
| Figure 4 Coomassie gel of purified RHOGDI proteins from <i>E. coli</i> expression system. A truncated version of GDI3 was purified to stabilize it but the data showed no difference. | 33 |
| Figure 5 Mass spectroscopy analysis of protein purified from insect cell system. | 34 |
| Figure 6 Crystal structure of GDI/RAC1 complex (PDB code: 1HH4)..... | 35 |
| Figure 7 Non-prenylated RAC1 bound with high affinity to GDI a-g..... | 36 |
| Figure 8 Displacement of liposome-bound prenylated RHO proteins by GDI1, 2 and 3. | 37 |
| Figure 9 Geranylgeranyl pyrophosphate (GGpp) does not inhibit GDI function over RAC1 ^{GG} | 37 |
| Figure 10 k_{obs} monitoring of interaction between fluorescent-labelled RHO proteins and GDI1 using stopped-flow measurement. | 38 |
| Figure 11 k_{obs} measurement of different prenylated, mant-dGDP-bound RHO GTPase toward GDI1 using stopped flow. | 39 |
| Figure 12 Polybasic residues contribute to GDI binding..... | 41 |
| Figure 13 Polybasic residues in HVR contribute to high affinity binding. | 42 |
| Figure 14 Liposome sedimentation of RAC1 ^{GG} in the presence of various GDI mutants. | 43 |
| Figure 15 Displacement of liposome-bound prenylated RHO by GDI..... | 46 |
| Figure 16 Liposome cycling of RAC mutant's was analyzed with SPR measurement. | 47 |
| Figure 17 GDI selectively displaced CDC42 from liposomes. | 48 |
| Figure 18 GDI binding of prenylated RHO GTPases. Prenylated RHO proteins were titrated to the surface of a GST-GDI immobilized CM5 chip in SPR. Obtained data are sorted in table 3. . | 49 |
| Figure 19 Affinity ratio of interaction of various RHO ^{GG} with GDI/membrane..... | 49 |
| Figure 20 Mass spectra analysis of CDC42 ^{lc} wild type and R186C mutant showed a strong peak in 24539 and 24486, respectively. | 51 |
| Figure 21 <i>In vitro</i> analysis of GDI function over wild type CDC42 and CDC42 R186C. a, GST-GDI pull down assay of CDC42 wild type and CDC42 mutant. | 52 |
| Figure 22 A representative surface plasmon resonance (SPR) analysis of GDI interaction with CDC42 wild type versus CDC42 ^{R186C} | 53 |
| Figure 23 Affinity of interaction of bodipy-coupled Rhonin versus different GDI concentrations indicated an affinity of 7.2 μ M. | 55 |
| Figure 24 Prenylated RAC1 interferes with Rhonin binding to GDI. | 55 |
| Figure 25 Analysis of inhibitory effect of Rhonin on GDI function over RHO GTPases..... | 56 |
| Figure 26 Surface plasmon resonance (SPR) measurement. | 57 |
| Figure 27 SPR analysis of Rhonin and its inactive variant 1025 on kinetic of GDI interaction with RAC1 ^{GG} | 57 |
| Figure 28 Proposed mechanism of GDI function as a membrane displacement factor..... | 63 |

List of tables

| | |
|---|----|
| Table 1 Bacterial strains used for protein expression. | 23 |
| Table 2 Primer sequences for cloning and protein expression. | 23 |
| Table 3 Direct binding of RHOGDI vs RHO proteins using antibody-GST chip coupled with GST-GDI..... | 43 |
| Table 4 Kinetic parameter of RHO GTPase membrane cycling. | 45 |

List of abbreviations

aa: Amino acid

CDC42: Cell division control protein 42 homolog

DH: Dbl-homology

DNA: deoxyribonucleic acid

DTT: dithiothreitol

E. coli: Escherichia coli

ER: Endoplasmic reticulum

Fig: Figure

FW: Forward

GDI: Guanosine nucleotide dissociation inhibitor

GEF: Guanine nucleotide exchange factor

GAP: GTPase-activating protein

GG: Geranylgeranyl

GGpp: Geranylgeranyl pyrophosphate

GGTase: Geranylgeranyl transferase

GDP: Guanosine-5'-diphosphate

GTP: Guanosine-5'-triphosphate

GST: Glutathione S-transferase

GTPase: Guanine triphosphatase

GSH: Reduced Glutathione

HVR: Hypervariable region

kDa: Kilodalton

mg: Milligram

min: Minute

ml: Milliliter

mM: Millimolar

mant-dGDP: 3'-O-(N-Methyl-anthraniloyl)-2'-deoxy-guanosine-5'-diphosphate

mant-GppNHp: (2'/3'-O-(N-Methyl-anthraniloyl)-guanosine-5'-[(β , γ)-imido]triphosphate

NaCl: Sodium Chloride

ND: not detected

Nm: Nanometer

NLS: Nuclear localization signal

PH: Pleckstrin homology

PS: Phosphatidylserine

PC: Phosphatidylcholine

PE: Phosphatidylethanolamine

PI(4,5)P₂: Phosphatidylinositol 4,5-bisphosphate

RAS: Rat sarcoma

RHO: RAS homolog

SDS: Sodium dodecyl sulfate

SOS1: Son of Sevenless 1

SPR: Surface plasmon resonance

SW: switch region

μ M: Micromolar

WT: Wild type

Amino acids abbreviation

| Name | Letter code | Name | Letter code | Name | Letter code | Name | Letter code |
|---------------|-------------|---------------|-------------|---------------|-------------|------------|-------------|
| Alanine | Ala (A) | Glutamic acid | Glu (E) | Leucine | Leu (L) | Serine | Ser (S) |
| Arginine | Arg (R) | Glutamine | Gln (Q) | Lysine | Lys (K) | Threonine | Thr (T) |
| Asparagine | Asn (N) | Glycine | Gly (G) | Methionine | Met (M) | Tryptophan | Trp (W) |
| Aspartic acid | Asp (D) | Histidine | His (H) | Phenylalanine | Phe (F) | Tyrosine | Try (Y) |
| Cysteine | Cys (C) | Isoleucine | Ile (I) | Proline | Pro (P) | Valine | Val (V) |

Summary

Studies in the last three decades have documented the role of guanine nucleotide dissociation inhibitor-1 (GDI1) in the regulation of spatio-temporal dynamics of RHO family GTPases. To tackle the unresolved interplay of kinetic mechanism and specificity, the GDI1-controlled spatial segregation of geranylgeranyl RHO GTPases was reconstituted *in vitro*, by calculating various biochemical and biophysical parameters, including on and off rates of RHO displacement from immobilized liposomes on the sensor chip of a surface plasmon resonance (SPR) instrument. Accordingly, our results showed: (1) An electrostatic mechanism determines interaction specificity between the C-terminal polybasic region of RHO GTPases and two distinct negatively charged clusters of GDI1. Thus, the GDI1-regulated displacement of RHO GTPases from the membrane underlies a 3-step mechanism. (2) A *de novo* missense mutation of CDC42, a member of the RHO GTPase family, disrupts electrostatic binding interface with GDI and thus causes a novel hematological and autoinflammatory disorder in humans. (3) A small molecule inhibitor of GDI1 interferes with the association of the geranylgeranyl moiety of RHO GTPases and causes RHO GTPase activation in response to hedgehog pathway. Collectively, this study considerably advances our knowledge about a selective function of GDI1 as a spatio-temporal regulator of RHO family GTPases.

Keywords: Displacement factors; electrostatic interaction; membrane cycling; RHO GTPases; spatio-temporal regulation; specificity.

Zusammenfassung

Studien in den letzten drei Jahrzehnten haben die Rolle des Guaninnukleotid-Dissoziationsinhibitors-1 (GDI1) in der Regulation der raumzeitlichen Dynamik von GTPasen der RHO-Familie dokumentiert. Um das bislang ungeklärte Zusammenspiel von kinetischem Mechanismus und Spezifität aufzuklären, wurde die GDI1-gesteuerte räumliche Trennung von geranylgeranylierten RHO GTPasen *in vitro* rekonstituiert. Hierbei wurden verschiedene biochemische und biophysikalische Messungen durchgeführt, einschließlich der geschwindigkeitskonstanten der Assoziation und der Dissoziation der RHO GTPasen von den auf einer Sensoroberfläche immobilisierten Liposomen mittels Oberflächenplasmonenresonanz (SPR). Dementsprechend ergaben die in dieser Studie durchgeführten Untersuchungen eine Reihe verschiedener Befunde: (1) Ein elektrostatischer Mechanismus bestimmt die Interaktionsspezifität zwischen der C-terminalen polybasischen Region von RHO-GTPasen und zwei verschiedenen negativ geladenen Clustern von GDI1. Somit unterliegt die GDI1-regulierte Verdrängung der RHO-GTPasen von der Membran einem 3-Schritt-Mechanismus. (2) Eine *de-novo*-Missense-Mutation von CDC42, einem Mitglied der RHO-GTPase-Familie, unterbricht die elektrostatische Bindungsschnittstelle mit GDI und verursacht somit eine neuartige hämatologische und autoinflammatorische Störung beim Menschen. (3) Ein kleinmolekularer Inhibitor von GDI1 interferiert mit der Assoziation der Geranylgeranyl-Einheit der RHO-GTPasen und verursacht eine RHO-GTPase-Aktivierung in Reaktion auf den Hedgehog-Stoffwechselweg. Zusammenfassend verbessert diese Studie unser Wissen über eine selektive Funktion von GDI1 als raumzeitlicher Regulator von GTPasen der RHO-Familie erheblich.

1.Introduction

1.1. RHO GTPase activation and function

The environment around cells is enriched by many chemical (cytokines) and physical (extracellular matrix and adhesions) stimuli that affect the cell morphology and function (Buchsbaum, 2007). In fact, cells receive the chemical/physical messages and make the optimal response to survive. Membrane receptors, like receptor tyrosine kinases and G-protein coupled receptors, mediate the transduction of signals from environment to the proper responses (Sah et al., 2000). Upon binding of ligand there is a cascade of conformational changes in downstream proteins which leads to the activation/inhibition of various signaling pathways and gene expression pattern (Neubig and Siderovski, 2002). Frequently, the activation of receptor leads to RHO signal transduction. RHO proteins control many essential processes, like proliferation, cytoskeleton dynamic, and cell polarity. Then, it is important to find out the spatio-temporal property of RHO activation process (Schwartz, 2004).

There are more than 20 RHO proteins in humans. The RHO family of GTPases is known to play an important role in diverse cellular processes and progression of different diseases, such as cardiovascular diseases, developmental and neurological disorders, as well as in tumor invasion and metastasis (Hall, 2012). RHO proteins exist in both form; cytosolic and membrane bound which could switch between GTP and GDP nucleotides states. Membrane binding ability is achieved by a hypervariable region (HVR) (Lam and Hordijk, 2013) and a lipid anchor in their C-terminal tail at a distinct cysteine residue in the CAAX motif (C is cysteine, A is any aliphatic amino acid, and X is any amino acid) (Philips and Cox, 2007; Roberts et al., 2008; van Hennik et al., 2003; Wennerberg and Der, 2004).

RHO protein function is dependent on its nucleotide binding states which affect its interaction toward various modifiers (Dvorsky and Ahmadian, 2004). This cycle underlies two critical intrinsic functions, the GDP-GTP exchange and GTP hydrolysis (Jaiswal et al., 2013b). RHO activation is controlled by at least three classes of regulatory proteins (Dvorsky and Ahmadian, 2004): i) Guanine nucleotide exchange factors (GEFs), which catalyze the exchange of GDP to GTP and activate the RHO protein (Jaiswal et al., 2013a; Rossman et al., 2005); ii) GTPase activating proteins (GAPs), which enhance the GTP hydrolysis and convey the RHO protein in its inactive conformation (Jaiswal et al., 2014; Tcherkezian and Lamarche-Vane, 2007); iii) Guanine

nucleotide dissociation inhibitors (GDIs), which bind to prenylated RHO proteins and extract them from membranes into the cytoplasm (DerMardirossian and Bokoch, 2005; Garcia-Mata et al., 2011; Tnimov et al., 2012).

1.2. Regulation of RHO GTPases

1.2.1. Guanine nucleotide exchange factor (GEF)

Guanine nucleotide exchange factors (RHOGEFs) are responsible for activation of RHO proteins in response of extracellular stimuli (Rossman et al., 2005). To survive, cell should communicate together and for this, they get information from their environment through either physical or chemical stimulus like cytokines, hormones and growth factors (Ghosh, 2015). Generally, cell surface receptors like cytokines, tyrosine kinase, adhesion and G-protein coupled receptors translate the external stimuli into the intracellular response via activation of specific GEF or GAP (Buchsbaum, 2007; Naor et al., 2000; Xie et al., 2017). There are more than 70 members of RHOGEFs that function specifically against various RHO proteins and lead to the regulation of divers cellular functions (Hall, 2005). RHOGEFs accelerate the intrinsic nucleotide exchange reaction of RHO GTPases from GDP-bound to GTP-bound form. Two groups of RHO GEF family are mostly responsible for nucleotide exchange as diffuse B-cell lymphoma (Dbl) family and a dedicator of cytokinesis (Dock). There are 74 Dbl GEF proteins containing a Dbl homology (DH) domain (Jaiswal et a., 2013). DH domain contains three conserved regions (CR1-CR3) which assemble together in the format of a GEF domain (Rossman et al., 2005).

Affinity of RHO proteins for nucleotide is in the range of pico/nano molar and intrinsic dissociation of nucleotide takes place in the range of hours and could not explain the signaling activation that occurs in minutes (Jaiswal et a., 2012). GEFs bind to RHO^{GDP} (their affinity is higher for GDP than GTP form) and decrease the affinity of nucleotide for RHO, which leads to dissociation of nucleotide. Then, due to the ten molar excess amount of GTP in comparison with GDP, RHO proteins bind to GTP and GEF will dissociate. G-protein bound nucleotide contains two regions called switch I and II which are making two loops for nucleotide binding (Dvorsky and Ahmadian, 2004). There is another region called p-loop and all these three regions coordinate phosphates of nucleotide and magnesium. Upon binding of GEF these three regions undergo a conformational change which leads to the reduction of nucleotide affinity for RHO (Bos et al., 2007).

1.2.2. GTPase-activating proteins (GAP)

There are more than 60 RHO GTPase-activating proteins (RHOGAPs) known in eukaryotes which regulate the inactivation process of RHO proteins. Some GAPs are characterized as specific RHOGAPs but most of the GAP function over RHO, RAC and CDC42 proteins (Amin et al., 2016; Tcherkezian and Lamarche-Vane, 2007). A large member of RHOGAPs could be explained with their specific functions as RHO downstream regulator in various cellular functions. In fact, to make a proper response, cells should turn on/off the given proteins in distinct position of cell. Specific GAP localization, activation and cell-type expression provides a clue for efficient regulation of cell functions (Tcherkezian and Lamarche-Vane, 2007). For instance, Rga1p in yeast is specific for CDC42 while Sac7p is a RHO1p specific GAP and it could explain the diverse functions of RHO in cell through specific regulation (Schmidt et al., 2002; Smith et al., 2002).

Activation of RHO should be tightly controlled and it has been shown that dysregulation of the RHO proteins makes them hyperactive which is a hallmark of cancer. Like nucleotide exchange ability of RHO, hydrolysis of GTP is very slow and does not cover the signaling demands. GAPs are the group of regulators that accelerate GTP hydrolysis. This reaction occurs through a arginine finger which stabilize the intermediates during the nucleotide hydrolysis (Bos et al., 2007; Fidyk and Cerione, 2002).

1.2.3. RHOGDI: structure and function

In contrast to a multitude of RHOGEFs (Jaiswal et al., 2013b) and RHOGAPs (Amin et al., 2016), there are only three genes encoding GDIs in mammals (Garcia-Mata et al., 2011) (Fig. 1). The RHOGDI family includes the ubiquitously expressed GDI1 (or RHOGDI α) (Xie et al., 2017), RHOGDI2 (RHOGDI β , LY-GDI or D4-GDI) mainly in hematopoietic tissue (Griner and Theodorescu, 2012), and GDI3 (or RHOGDI γ) that is usually expressed in human cerebral, lung and pancreatic tissue (de Leon-Bautista et al., 2016). Unlike the other two GDIs, GDI3 contains an LDXXEL motif that confers anchorage into the outer leaflet of Golgi membranes (Brunet et al., 2002). In addition to their physiological expression, GDIs are also overexpressed/or downregulated in several human cancers, including breast, liver, ovarian, pancreatic cancers, and myeloid leukemia (Garcia-Mata et al., 2011; Griner and Theodorescu, 2012; Harding and Theodorescu, 2010; Xiao et al., 2014). Changes in GDI expression levels have shown pro- or anti-

tumorigenic effects that depend on the cell type and tissue. One reason for this debate is most probably due to the lack of our understanding of the basic mechanism of the GDI function and their binding specificities to the different RHO proteins.

Comprehensive studies in the last two decades provided valuable insights into structure and function of GDI1 as a shuttle for the RHO proteins (DerMardirossian and Bokoch, 2005; Garcia-Mata et al., 2011; Hodge and Ridley, 2016). The shuttling process involves extraction of RHO proteins from donor membranes, formation of inhibitory cytosolic GDI-RHO protein complexes, and delivery of RHO proteins to target membranes (DerMardirossian and Bokoch, 2005; Garcia-Mata et al., 2011). Sequestering RHO proteins from the membrane maintains them in an inactivated state, protects against both degradation and unspecific activation by RHOGEFs (Garcia-Mata et al., 2011; Robbe et al., 2003; Zhang et al., 2014). Structural studies by different groups have provided first insights into the two main sites of interaction between GDI and RHO proteins (Dransart et al., 2005; Grizot et al., 2001; Hoffman et al., 2000; Longenecker et al., 1999; Scheffzek et al., 2000). First, the amino-terminal regulatory arm of GDI binds to the switch I and II domains of CDC42 leading to the inhibition of both GDP dissociation and GTP hydrolysis. Second, the geranylgeranyl moiety of CDC42 inserts into a hydrophobic pocket within the immunoglobulin-like domain of the GDI molecule leading to membrane release. How GDIs interact with and serve as negative regulators of RHO proteins has been clearly demonstrated by these structural analyzes, however the basic mechanisms of how they pull the isoprenoid moiety from the membrane or how the RHO protein is released from the complex remained unresolved. There are several modulators proposed to fulfill these functions. Proposed GDI displacement factors include the neurotrophin receptor p75 (p75^{NTR}) and Troy (Lin et al., 2015; Lu et al., 2013; Yamashita and Tohyama, 2003), and members of the ezrin/radixin/moesin (ERM) protein family (Takahashi et al., 1997). Other factors that directly modulate the GDI functions are phospholipids, such a phosphoinositide (3,4,5)-trisphosphate (PIP₃) (Ugolev et al., 2008). Nevertheless, the mechanistic details of such GDI modulators or displacement factors remain unclear. Furthermore, many of *in vitro* studies performed in the absence of membrane that is an essential step toward cellular function GTPases (Nalbant et al., 2004).

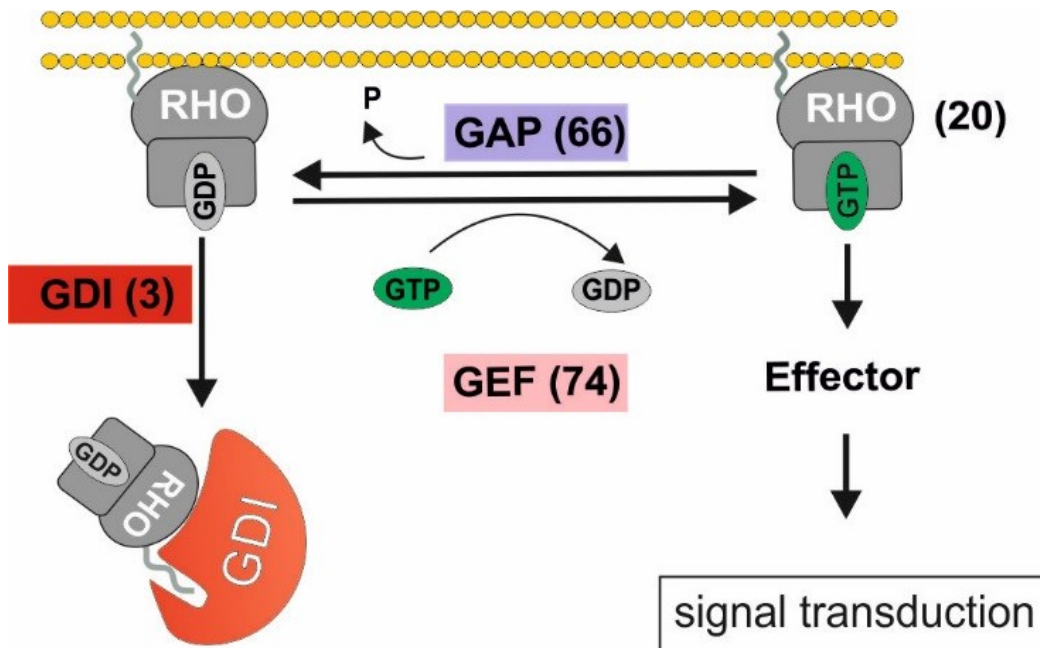


Figure 1 General activation cycle of RHO GTPases. There are three classes of regulators controlling RHO GTPase activation cycle. More than 70 GEF proteins stimulate nucleotide exchange of RHO and more than 60 GAP proteins stimulate GTP hydrolysis. There are three RHOGDIs in human regulating membrane shuttling of RHO proteins. Activated RHO interacts with a wide range of effector proteins and leads to downstream signaling.

1.2.4. RabGDI

Rab guanosine nucleotide dissociation inhibitor (RabGDI) is a member of GDI family, which specifically regulates the membrane trafficking of Rab GTPase family. Rab proteins are the largest family of small GTPase with more than 60 members and play a central role in vesicle membrane trafficking (Ignatev et al., 2008). Rab proteins are following the same switch mechanism between GTP and GDP nucleotide forms and get prenylated (mostly in two sites) by addition of geranylgeranyl moieties, which enable them to anchor to the membrane. RabGDI functions nucleotide dependent and regulate the displacement of proteins (Ignatev et al., 2008; Pereira-Leal and Seabra, 2001).

Based on crystal structure analysis, RabGDI binds Rab via three distinct regions; GDI-Rab binding platform (RBP), C-terminus coordinating region (CCR), and hydrophobic binding pocket which is the geranylgeranyl insertion site (Rak et al., 2003). Following the proposed mechanism, RabGDI

primarily binds by its RBP to membrane bound Rab with macromolar affinity and CCR stabilizes the complex through binding to C-terminus of Rab. Finally, geranylgeranyl lipid will transfer to hydrophobic pocket of RabGDI and form a complex with nanomolar affinity which displaces Rab from the membrane (Ignatev et al., 2008).

1.3. Posttranslational modification

1.3.1. Prenylation of RHO GTPases

Prenylation is a posttranslational that processes by addition of isoprenoid moiety to the proteins, which makes them labeled for membrane localization. Generally, this process needs a CAAX code on the target proteins for addition of farnesyl or geranylgeranyl moieties (Wang and Casey, 2016). This specific region is a code for posttranslational modification of proteins via addition of a isoprenoid moiety like geranylgeranyl or farnesyl chains (Gao et al., 2009). C stands for a Cysteine residue and AA indicates to aliphatic residues. RAS superfamily proteins contain a CAAX box code at the very C-terminal tail. Process of prenylation of RHO and RAS proteins occurs by two classes of cytosolic enzymes named geranylgeranyl (GGTase I) and farnesyl transferases (FTase), respectively (Wang and Casey, 2016).

Isoprenoids are build up out of isoprenoid building blocks, which are downstream product of the mevalonate pathway. GGTase I and FTase bound to the prenyl-moiety in cytosol and then bind to CAAX region (Wang and Casey, 2016). The process occurs by insertion of geranylgeranyl moiety into the hydrophobic pocket of GGTase following the interaction of CAAX box containing RHO. Then, GGTase binds to the outer leaflet of endoplasmic reticulum where two other enzymes exist for further catalysis. Later, the C-terminus of RHO is processed via digestion of AAX sequence by an endopeptidase (RCE1) and methylation of prenylated cysteine by isoprenylcysteine carboxylmethyltransferase (ICMT) (Wang and Casey, 2016).

Prenylation regulates various cellular processes. Binding of geranylgeranyl (RAC1-3, CDC42 and RHOA) or farnesyl groups (RHOB) traffics RHO to the membrane (Allal et al., 2002; Baron et al., 2000). Inhibition of prenylation could inhibit cell proliferation by blocking the farnesylation of HRAS, which inhibit the membrane targeting of the protein (Liu et al., 2010). It has been shown that inhibition of farnesylation could arrest the cancer cells in G1 or G2 phase in a p53 dependent manner (Ashar et al., 2001).

1.3.2. Phosphorylation and acetylation of GDI

There are few factors like phosphorylation, acetylation and prenylation that regulate GDI function and provide specific interaction toward various RHO proteins. On the one hand, Phosphorylation of GDI has a huge impact on its interaction with RHO proteins. For instance, phosphorylation of GDI (at positions of 101 and 174) by PAK reduces its affinity for RAC1 and shifts it to RHOA (DerMardirossian et al., 2004). Additionally, phosphorylation of RHOGDI by Src at position of Tyr156 reduces the affinity of the GDI interaction toward CDC42, RHOA and RAC1 (DerMardirossian et al., 2006). GDI2 phosphorylation at Ser31 also reduces its affinity toward RAC1 (Griner et al., 2013). On the other hand, phosphorylation of RHO proteins via kinases could also affect this mechanism. For example, RHOA phosphorylation at Ser188 leads to an increased binding affinity for RHOGDI that causes cytosolic localization of RHOA (Ellerbroek et al., 2003; Forget et al., 2002). Beside phosphorylation as a regulating factor, RHOGDI could get acetylated in at least 8 different positions such as; Lys-43, Lys-52, Lys-99, Lys-105, Lys-127, Lys-138, Lys-141, and Lys-178. Depending on the position, these acetylations regulate RHO proteins function and indirectly affect cytoskeleton organization (Kuhlmann et al., 2016).

1.4. Impact of membrane lipids on RHO signaling

The membrane contains various lipid contents, which give electrostatic, curvature, rigidity, and different levels of hydrophobicity to the membrane. Some lipids are shown to be important for signal transduction through localizing specific proteins in a close vicinity of different membranes like plasma membrane, Golgi, mitochondria, endoplasmic reticulum, and nucleus (Lam and Hordijk, 2013; van Hennik et al., 2003). Then, lipid bilayer plays a critical role in activation of RHO protein through interaction, activation and localization of GEFs. PIP₂ is a target for the proteins containing pleckstrin homology (PH) domain like Tiam1, β -Pix, P-Rex1. Reconstitution of RAS activation via synthetic liposomes has shown that PIP₂ is important for activation of RAS GEF protein SOS1 as well (Gureasko et al., 2008). Interaction of GEF PH domain with membrane PIP₂ could lead the conformations of PH and DH domains which release and uncover the GEF domain and increase its activity (Worthylake et al., 2004). Furthermore, there is a long discussion about formation of lipid domains, which could provide a code for localization of specific proteins leading to partitioning of different signaling cascades in various positions in the cell (Karnovsky et al., 1982; Varshney et al., 2016). RHO GTPases are prenylated in the endoplasmic reticulum and are

transported to the different membranes. They have also various frequencies of positively charged residues at the C-terminal part, which provides an electrostatic interface and it has the potential to interact with negatively charged lipids like PIP2 and phosphatidylserine localized into the inner leaflet of membrane. RAC1 contain a sequence of 6 positive charges in a part of HVR called polybasic region (Lam and Hordijk, 2013; van Hennik et al., 2003).

Aims

In this study, we analyzed the mechanism of GDI function in order to understand its specificity toward various RHO proteins and provide a detail view of the spatio-temporal regulation of RHO GTPases. We proposed an electrostatic model supported by kinetic analysis of GDI interaction toward RAC1. Specificity of GTPases interaction with GDI, and rate limiting steps in membrane displacement are central factors to understand the nature of GDI function *in vitro*. We were also able to formulate a matrix of binding residues based on crystal structures, which are supported by interaction studies on C-terminal part of GTPases and N-terminal part of GDIs. Crystal structures showed a flexible N-terminal part in GDI, which placed around ten angstrom away from HVR of RHO GTPases (Grizot et al., 2001; Scheffzek et al., 2000). Our proposed model shifts the paradigm of un-selective GDI/GTPase interaction toward a selective mechanism of interaction by focusing on missing information in the positively charged C-terminal region of GTPases and negatively charged N-terminal region of GDI.

2. Material and methods

2.1. Constructs

Human *Rac1* (GenBank accession no. NM_006908.4), *Rac2*, *CDC42*, *RHOA* were subcloned into pFastBacHTB vector (Invitrogen, Carlsbad, CA) and fused with an N-terminal hexa-histidine (6xHis) tag (Tables 1 and 2). For bacterial expression, full-length, mutant and C-terminal truncated *Rac1* and all other RHO GTPases including *RAC2*, *RAC3*, *CDC42*, *RHOA-C*, *RIF*, *TCL* and *TC10* plus *GDI1-3* (GenBank accession no. D13989) were cloned into pGEX-4T1 vector.

Table 1 Bacterial strains used for protein expression.

| Bacterial strain | Genotype | Supplier |
|------------------------------------|---|--|
| <i>E. coli</i> BL21 (DE3) pLysS | F ⁻ , <i>ompT</i> , <i>hsdS_B</i> (<i>r_B</i> ⁻ , <i>m_B</i> ⁻), <i>dcm</i> , <i>gal</i> , λ(DE3), pLysS, Cm ^r . | Promega, Madison, WI, USA |
| <i>E. coli</i> Rosetta (DE3) | F ⁻ <i>ompT</i> , <i>hsdS_B</i> (<i>r_B</i> ⁻ , <i>m_B</i> ⁻), <i>gal dcm</i> (DE3), pRARE (Cm ^R) | Merck, Darmstadt, Germany |
| <i>E. coli</i> Codon Plus | | |
| <i>E. coli</i> XL1-Blue | <i>recA1 endA1 gyrA96 thi-1 hsdR17 supE44</i> <i>relA1 lac</i> [F' <i>proAB lacI</i> ^q Zdelta-M15 Tn10, (Tet ^r)]. | Agilent Technologies, Santa Clara, CA, USA |

Table 2 Primer sequences for cloning and protein expression.

| Gene | Forward primer | Reverse primer |
|---------------------------|---|------------------------------------|
| RhoGDI163KK-F | GTTCTGACCCCCGTGAAGAAGGCACCCAAGGGTATGC | EE163/164KK |
| RhoGDI163KK-R | GCATACCCTTGGGTGCCTTCTTCACGGGGGTCAGGAAC | EE163/164KK |
| Rac1-5E-F | CCCGCCTCCCGTGAAGGAAGAGGAAGAGGAATGCCTGCTGTTGTAAG | Rac1 KRKRK to EEEEE |
| Rac1-5E-R | CTTACAACAGCAGGCATTCCTCTTCTCTCTCTTCACGGGAGGCGGG | Rac1 KRKRK to EEEEE |
| RhoGDIdelta25N-F | CGGGATCCAACTACAAGCCCCGGCCC | RhoGDI N terminus delta25 BamHI |
| RhoGDIdelta15N-F | CGGGATCCGCGGAGAACGAGGAGGATG | RhoGDI N terminus delta15 BamHI |
| RhoGDIdeltaN-R | CCGCTCGAGTCAGTCCTTCCAGTCCTTC | RhoGDI reverse XhoI |
| RhoGDIdelta25N-F- NcoI | CATGCCATGGCTAACTACAAGCCCCGGCCC | RhoGDI N terminus delta25 NcoI |
| RhoGDIdelta15N-F- NcoI | CATGCCATGGCGGAGAACGAGGAGGATG | RhoGDI N terminus delta15 NcoI |
| GDI3-F | CGGGATCCATGCTGGGCCTGGACGCG | BamHI for pGEX4T1NTEV |
| GDI3-R | CCGCTCGAGTCAGTCCTTCCAGTCCTG | xhoI for PGEX4T1NTEV |

*mutations showed in red color.

2.2. Softwares and programs

Following programs, versions and web-based tools used in this study:

Biacore X100 Evaluation Software Version 2.0.1 (GE Healthcare, Freiburg, Germany)

EndNote X7 (Thomas Reuter, Carlsbad, CA, USA)

GraFit 5 (Erithacus Software Limited, Surrey, UK)

Microsoft Office 2013 (Microsoft Corporation, Redmond, USA)

PyMOL (Richardson Lab, Duke University, NC, USA)

SnapGene (GSL Biotech LLC, Chigago, IL, USA)

2.3. Antibodies, media and reagents

Anti-His-tag (mouse), anti-RAC (mouse), anti-GDI (mouse), anti-CDC42 (mouse), anti-GST (rabbit) and anti-RHOA (rabbit), were purchased from Invitrogen (Oregon, USA). Anti-mouse IgG was obtained from Dako (rabbit, California, USA). GDP and a non-hydrolyzable GTP analogue, guanosine 5'-[β,γ -imido]triphosphate (GppNHp), mant-GppNHp (2'/3'-O-(N-Methyl-anthraniloyl)-guanosine-5'-[β,γ -imido]triphosphate, Triethylammonium salt), and mant-dGDP (3'-O-(N-Methyl-anthraniloyl)-2'-deoxyguanosine-5'-diphosphate, Triethylammonium salt) were obtained from Jena Bioscience GmbH (Jena, Germany). SF9 III insect cell media, Grace antibiotic free SF9 media and antibiotics (penicillin and streptomycin) purchased from Thermofisher (Germany). Phosphatidylserine (PS), Phosphatidylcholine (PC), phosphatidylethanolamine (PE), cholesterol and phosphatidylinositol 4,5-bisphosphate (PIP₂) were obtained from Avanti (Germany). PIP₃ is from Merck (Darmstadt, Germany). All other standard reagents, including detergents were obtained from Carl Roth GmbH (Karlsruhe, Germany) and Merck-Millipore (Darmstadt, Germany).

2.4. Baculoviruses and insect cell culture

Human *Rac1*, *Rac2*, *RhoA* and *CDC42* genes were subcloned into the pFastBacHTB vector (Invitrogen, Carlsbad, CA) and transformed into the DH10BAC strain of *E. coli*. Agar plates containing kanamycin, gentamycin, tetracycline, X-gal and isopropyl- β -D-thiogalactoside were used to select recombinant *GTPases* clones. The GTPase-positive clones were selected and

isolated with midiprep for recombinant *GTPase* bacmid extraction and virus generation. The baculoviruses (passage 1) were generated by infecting *Sf9* insect cells using recombinant *GTPase* bacmids. Viruses have been used for large scale *Rac1*, *Rac2*, *RhoA* and *CDC42* expression, after two amplification steps (passages 2 and 3). For a large scale medium, *TNAO38* were used due to the high efficiency compare with *Sf9*. *Sf9* and *TNAO38* were cultured in SF9 III medium, containing penicillin and streptomycin at 27°C. The multiplicity of infection (MOI) and RHO expression time were optimized by infecting the *Sf9* cells at different time points. A sample of transfected culture was analyzed with immunoblotting using an anti-His-tag antibody.

2.5. Protein purification and nucleotide exchange

Large scale *insect cell* expression of RHO proteins were conducted according to the established protocol described before (Zhang et al., 2014). *Sf9*/or *TNAO38* insect cells were inoculated at a density of 1.5×10^6 cells/ml under optimized virus titration and culture time. Cells were resuspended in lysis buffer, containing 20 mM HEPES-NaOH pH 7.4, 150 mM NaCl, 2 mM β -mercaptoethanol, 5 mM $MgCl_2$, 0.1 mM GDP, 10 mM imidazole and the optimized detergents (Zhang et al., 2014). Cells were cracked using sonication in ice. Supernatants were collected by centrifugation and loaded on a Ni-NTA superflow column (Qiagen, Hilden, Germany). Hypertonic buffer (20 mM HEPES-NaOH pH 7.4, 150 mM NaCl, 2 mM β -mercaptoethanol, 5 mM $MgCl_2$, 0.1 mM GDP, 10 mM imidazole, 350 mM KCl and 1 mM ATP) was used to remove unspecific-bound impurities from the proteins of interest. Target protein was eluted using 300 mM imidazole containing buffer. The eluted solution was concentrated and further purified on a Superdex 75 column (10/300 GL, GE-Healthcare, Uppsala, Sweden) with 20 mM HEPES-NaOH pH 7.4, 150 mM NaCl, 3 mM DTT, 5 mM $MgCl_2$ and 0.5% (w/v) Na-cholate as buffer system. All other GTPases including C-truncated constructs as well as human GDIs and mutants were purified from *E. coli* as a GST recombinant proteins (Figs. 3 and 4).

2.6. Mass Spectrometry

Deconvoluted mass spectra of RHO proteins are shown in figure 5. RHO proteins, purified from *TNAO38* insect cells, were dissolved in 50% (v/v) acetonitrile and 0.2% (v/v) formic acid at a final

concentration of 2 mg/ml. Proteins were subjected to a C4 HPLC column (MassPrep Online Desalting Cartridge, dimensions 2.1*10mm, Waters, Germany) equilibrated with 20 % (v/v) acetonitrile and 0.1 % (v/v) formic acid. The following conditions were used for HPLC separation: HPLC-system U300 series (Agilent Technology, Waldbronn, Germany), a flow rate of 500 µl/min, eluent A: 0.1 % (v/v) formic acid in water, eluent B: 0.1 % (v/v) formic acid in acetonitrile, gradient conditions: 20 % B for 0.5 min, linear gradient up to 60 % B in 1.5 min, linear gradient up to 90 % B in 0.5 min, 90 % B for 0.5 min, reequilibration of the column. The HPLC-system was coupled on-line to an ion trap mass spectrometer (VelosPro, Thermo Fisher Scientific, Germany) equipped with an electrospray ionization source. Full spectra were acquired using a mass-to-charge range of 700 to 2000. Obtained spectra were deconvoluted using the program package Promass (Thermo Fisher Scientific, Germany). Masses obtained from the respective spectra are described with respect to calculated molecular weights (MW). CH₃, methyl group; Da, Dalton; lc, insect cells; GG, geranylgeranyl moiety

2.7. Liposome preparation

Liposome assay were performed by mixing, sonication and extruding the define amount of various lipids. The lipid mixtures were incubated for different time points and centrifuged at different speeds to optimize the separation of pellets and supernatants. The liposomes were prepared as described previously (Zhang et al., 2014). A lipid mixture (500 µg), containing 20% (w/w) PE, 45% (w/w) PC, 20% (w/w) PS, 10% (w/w) cholesterol, and 5% (w/w) PIP₂, was gently dried using light air stream at the bottom of 2 ml microcentrifuge vial. Obtained lipid film was hydrated with 300 µl of a buffer, containing 20 mM HEPES-NaOH pH 7.4, 50 mM NaCl, 3 mM DTT, 5 mM MgCl₂. Sonication (20 s with minimal power, 50% off and 50% on) was used to dissolve the lipids and promote aggregates formation. At the end, to homogenize the liposome size we used 200 nm filters in extruders and filters the sample for 21 injects.

Calculation of RAC1 molecule per liposome

Surface capacity of a vesicle = $4\pi r^2 \approx 4 \times 3.14 \times 100^2 \text{ nm} = 125.600 \mu\text{m}^2$

Number of lipids per vesicle = Surface lipids + inner layer lipids = $(4 \times 3.14 \times 100^2 \text{ nm}) + (4 \times 3.14 \times 98^2)$ (Radius of inner layer of vesicle $\approx 98 \text{ nm}$) = $125.6 + 120.6 = 246.2 \text{ } \mu\text{m}$ total area

Surface area of lipid $\approx 0.8 \text{ nm}^2$

Number of lipids per vesicle outer layer surface $\approx 24.6 \times 10^4 / 0.8 = 307750$ (number of lipids per liposome)

*average molecular weight of lipids was 626 Da

*lipid concentration in solution = $500 \text{ } \mu\text{g} / 300 \text{ } \mu\text{l} = 1 \text{ gr/lit} = 1 / 625 = 1.5 \text{ mM}$

Number of RAC1 protein per vesicle with 100 nm radius = number of RAC1 (Avogadro number \times %mol RAC1 found in liposomal fraction) \times number of liposome (number of lipids/lipids per vesicle) $\approx (1 \times 10^{-6}) \times (6.022 \times 10^{23}) / ((1.5 \times 10^{-3}) \times (6.022 \times 10^{23})) / 307750 \approx 6.022 \times 10^{17} / 2.9 \times 10^{15} = 207 \text{ RAC1}^{\text{GG}}$ molecules/vesicle.

*Based on sedimentation assay 2/3 of total RAC1 is bound to the liposome (Fig. 9). Then, 138 molecules of RAC1 ($2/3 \times 207 = 138$) are theoretically bound to each liposome.

2.8. Kinetics of the protein-protein interaction

2.8.1. Stopped flow measurement

In order to monitor the kinetic behavior of GDI interaction with full-length RHO proteins, stopped flow measurements performed. Using this method, we were able to measure association rate constant (k_{on}) and dissociation rate constant (k_{off}). k_{on} value was measured by monitoring association of mant-dGDP RHO proteins with increasing concentrations of GDI. k_{obs} was fitted in a linear mode as a function of GDI concentrations and the slope of fitted line provides the k_{on} values. Displacement of GDI from fluorescently labeled RHO proteins measured by rapid mixing of the mant-dGDP RHO proteins in complex with the GDI1 with an excess amount of non-fluorescent GDP RHO proteins. From the rate constant ratio of $k_{\text{off}}/k_{\text{on}}$ we are able to calculate dissociation constant (K_d). For these measurements, we used a stopped-flow instrument (Hi-Tech Scientific SF-61 with a mercury xenon light source and TgK Scientific Kinetic Studio software). It was operates fully automated and allows collection of up to 1000 data points within a time window

of 100 ms to 400 s. Principally, equal volumes of two solutions are pumped into a mixing chamber and fluorescence signal is monitored. To obtain a high accuracy several identical measurements are recorded and averaged signal was selected for fitting.

2.8.2. Fluorescence polarization

To investigate the binding of RAC1 to the GDI, fluorescence polarization of the mant-dGDP RAC1 was monitored. The 2 μ M fluorescently labelled RAC1 was added to the cuvette containing buffer (30 mM Tris, pH 7.5, 50 mM NaCl, 3 mM DTE). Increasing amount of GDI1 protein was added to the cuvette to saturate the system. The change in the fluorescence polarization was monitored at the excitation and emission wavelengths of 360 nm and 450 nm corresponding to RAC1-mant-dGDP. Data analysis was done with GraFit 5.0 program (Erithracus Software). To monitor bodipy-coupled compound, excitation and emission wavelengths of 535 nm and 593 nm were set.

2.9. Liposome reconstitution of RHO protein displacement by GDI

2.9.1. Sedimentation assay

Materials: Buffer contains 20 mM HEPES, pH 7.4, 50 mM NaCl, 5 mM $MgCl_2$, 3 mM DTT. Briefly, liposomes were generated by using a defined composition of lipids (500 μ M), containing 10 % (w/w) phosphatidylethanolamine, 45 % (w/w) phosphatidylcholine, 20 % (w/w) phosphatidylserine, 10 % (w/w) Cholesterol, and 5 % (w/w) Phosphatidylinositol 4,5-bisphosphate.

Method: Displacement of modified RHO from synthetic liposomes by GST-GDI1 was analyzed using liposome sedimentation assay (Zhang et al., 2014). Modified RHO^{GG} added to the liposomes solution (20 mM HEPES, pH 7.4, 150 mM NaCl, 3 mM DTT) and incubated for 20 min on ice. Later, GST-GDI1 was added to the liposome. Next, samples were centrifuged at 20000 g for 20 min at 4 °C and the obtained pellet and supernatant were prepared for western blotting.

2.9.2. Flotation assay

Materials: Buffer contains 20 mM HEPES, pH 7.4, 50 mM NaCl, 5 mM MgCl₂, 3 mM DTT. Liposomes were generated using a defined composition of lipids (500 μM), containing 5 % (w/w) phosphatidylethanolamine, 45 % (w/w) phosphatidylcholine, 20 % (w/w) phosphatidylserine, 10 % (w/w) Cholesterol, 5 % (w/w) Phosphatidylinositol 4,5-bisphosphate, and 5% NDB-phosphatidylethanolamine (NDB-PE).

The displacement of modified RHO from synthetic liposomes by GST-RHOGDI1 in the presence and absence of compound was further analyzed using liposome floatation assay, which described before (Bigay et al., 2005). In order to avoid the possible errors due to precipitation liposome-bound proteins applied to a gradient centrifugation. Modified RHO^{GG}-GDP added to the liposomes and incubated for 20 min on ice. GST-GDI1 was added to the liposome-bound RHO sample and further incubated on ice for 30 min. The samples were added to the 200 μL buffer with 30 % v/v sucrose. Then, it was overlaid with 150 μL 25% v/v sucrose buffer and on the top, 50 μL buffer without sucrose. The resulting samples were centrifuged at 200,000g for 1 h at 4 °C. The upper liposome-containing phase (detected by 5% fluorescent NDB-PE) was collected and analyzed by western blotting.

2.10. Surface plasmon resonance analysis

2.10.1. GDI direct interaction with RHO

Materials: buffer contains 20 mM HEPES-NaOH pH 7.4, 150 mM NaCl, 5 mM MgCl₂, and surfactant P20 provided by (GE Healthcare). CM5 chip was used for immobilization of GST-GDI using GST capture kit (GE Healthcare).

Biacore X100 instrument (Biacore, GE Healthcare) was used to analyze the direct interaction of RHO protein with immobilized GST-GDI. GST-GDI was immobilized on surface of CM5 chip coupled with anti-GST antibody and later, increasing concentrations of RHO proteins were injected with the rate of 30 μL/min in a time course of 90 s and a single cycle mode. Dissociation of RHO from immobilized GST-GDI was also measured by injection of buffer at the last step for a period of 600 s. To analyze data, the final curve was fitted to a 1:1 binding mode.

2.10.2. RHO interaction with liposome

Materials: buffer contains 20 mM HEPES-NaOH pH 7.4, 150 mM NaCl, 5 mM MgCl₂, and surfactant P20 provided by GE Healthcare. For liposome binding analysis, we used L1 was used.

Liposomes were immobilized by injecting 0.5 mM liposomes (5µL/min) in buffer on the surface of a L1 sensor chip (GE Healthcare) for the period of 900 s, as indicated by a constant signal. The unbound liposomes were removed by introducing a buffer of NaOH (10 mM) with the rate of 30 µL/min for 30 s over sensor chip. Next, RHO^{GG} proteins were flow (30 µL/min) over the immobilized liposomes in a multi cycle mode. Then, buffer flow to the system to measure the dissociation of RHO from liposome. To analyze data, the final curve was fitted to a 1:1 binding mode.

2.11. GST-GDI pull down assay

Materials: buffer contains 20 mM HEPES-NaOH pH 7.4, 150 mM NaCl, 5 mM MgCl₂, 3 mM DTT. GSH beads (GE healthcare).

Method: GST beads were washed three times with buffer and incubate for 30 min with 30 µM GST-GDI. 1 ml solution of 20 µM CDC42 wild type and mutant was added to the GSH bead and further incubate for 30 min. later, samples were centrifuged and the beads washed three times. Beads were incubating with leading dye and incubated 10 min in heat block machine for western blotting.

3. Results

3.1. Chapter I: GDI mechanism of function

3.1.1. Kinetics of the GDI/RHO protein interactions

There are many GEFs and GAPs for regulation of 20 members of RHO GTPase family but just one ubiquitously expressed GDI exist in mammals (GDI1) (REF). Our challenge is first, why nature made just one ubiquitously expressed GDI for regulation of 20 various RHOs and second,

how one GDI is able to distinguish between this diversity. Because of the central role of GDI as a hemostatic factor for active and inactive populations of RHO proteins and its role as a localizing factor, which regulates RHO proteins cycling between endomembrane, plasma membrane and cytosol, we proposed a specific function for GDI, which in this case, could explain specific activation of RHO.

Based on resolved crystal structures (REF), we have launched a matrix to analyze the interface between RHOs and GDIs (Fig. 2). Numbering of ligament is based on the RAC1 and GDI1 sequences. This model showed that the residues, which are involved in binding interfaces, remain almost conserved within RHOs and GDIs. For example, R66, R64, and geranylgeranyl moieties from RHO making two central interfaces of the complex and interact with D184, W194 residues of GDI. The matrix shows that these regions are highly conserved (Fig. 2).

To understand the mechanism of GDI interaction with RHO proteins, we purified non-prenylated and prenylated RHO proteins in order to analyze the impact of geranylgeranyl moiety on GDI interaction. Geranylgeranyl moiety is conserved for RHOA, RAC1-2 and CDC42. In addition, it showed the largest binding interface with GDI (REF). Prenylated proteins purified from insect cell and characterized by mass spectrometry. Deconvolution and analyzing of the mass spectra showed the geranylgeranylation of RHO proteins (RHOA, RAC1, CDC42 and RAC2) (Fig. 5). Non-prenylated proteins were also purified from *E. coli* system (Figs. 3 and 4). Based on previous studies, GDI could interact with both nucleotide-bound forms (GDP/GTP) of RHO proteins but the binding affinity is higher for GDP form of RHO (Garcia-Mata et al., 2011).

Current model of GDI interaction with RHO proteins (RAC2, CDC42, RHOA and RAC1) suggests an unspecific interaction between RHO and GDI, which occurs in nanomolar ranges (Garcia-Mata et al., 2011; Nomanbhoy et al., 1999; Pertz et al., 2006; Ugolev et al., 2008). Crystal structures show a conserved binding interface between various RHO proteins and GDI which exist between the geranylgeranyl moiety of RHO and the hydrophobic pocket of GDI as well as switch II region of RHO (mostly through residues R68 and R64) and C-terminus of GDI (Fig. 6) (Grizot et al., 2001; Longenecker et al., 1999; Scheffzek et al., 2000). Kinetic models also propose two-phases of interaction, which start with a fast association of N-terminus of GDI with RHO followed by slow displacement of geranylgeranyl moiety from membrane into the hydrophobic pocket (Dovas and Couchman, 2005; Nomanbhoy et al., 1999).

| | | 27 | 30 | 31 | 32 | 33 | 41 | 42 | 45 | 48 | 50 | 51 | 52 | 55 | 56 | 122 | 125 | 145 | 148 | 149 | 150 | 184 | 185 | IDs2 | | | |
|------|-------|----|----|----|----|----|----|----|----|----|----|----|----|----|----|-----|-----|-----|-----|-----|-----|-----|-----|------|--------|----|----|
| | GDI2 | Y | P | P | Q | K | M | D | D | S | L | K | Y | K | L | L | I | G | M | S | Y | G | D | D | P52566 | | |
| | GDI1 | Y | P | A | Q | K | L | D | D | S | L | K | Y | K | L | L | I | G | M | S | Y | G | D | D | P52565 | | |
| | GDI3 | Y | P | G | R | K | L | D | D | S | L | K | Y | K | L | L | I | G | M | S | Y | G | D | D | Q99819 | | |
| | GDI1 | Y | P | A | Q | K | L | D | D | S | L | K | Y | K | L | L | I | G | M | S | Y | G | D | D | P19803 | | |
| | GDI1 | Y | P | A | Q | K | L | D | D | S | L | K | Y | K | L | L | I | G | M | S | Y | G | D | D | Q99PT1 | | |
| 34 | P | P | P | P | P | P | P | P | P | P | | | | | | | | | | | | | | | 7 | 5 | |
| 35 | T | T | T | T | T | T | T | T | T | T | | | | | | | | | | | | | | | | 7 | 4 |
| 36 | V | V | V | V | V | V | V | V | V | V | | | | | | | | | | | | | | | | 0 | 0 |
| 38 | E | E | E | D | D | D | D | D | D | D | | | | | | | | | | | | | | | | 0 | 0 |
| 57 | D | D | D | D | D | D | D | D | D | D | | | | | | | | | | | | | | | | 12 | 4 |
| 58 | T | T | T | T | T | T | T | T | T | T | | | | | | | | | | | | | | | | 7 | 9 |
| 59 | A | A | A | A | A | A | A | A | A | A | | | | | | | | | | | | | | | | 8 | 7 |
| 60 | G | G | G | G | G | G | G | G | G | G | | | | | | | | | | | | | | | | 9 | 9 |
| 63 | D | D | D | D | D | D | E | D | D | D | | | | | | | | | | | | | | | | 6 | 12 |
| 64 | Y | Y | Y | Y | Y | Y | Y | Y | Y | Y | | | | | | | | | | | | | | | | 6 | 4 |
| 65 | D | D | D | D | D | D | D | D | N | D | D | | | | | | | | | | | | | | | 8 | 3 |
| 66 | R | R | R | R | R | R | R | R | Q | R | R | | | | | | | | | | | | | | | 9 | 6 |
| 67 | L | L | L | L | L | L | L | L | L | L | | | | | | | | | | | | | | | | 5 | 5 |
| 68 | R | R | R | R | R | R | R | R | R | R | | | | | | | | | | | | | | | | 0 | 0 |
| 69 | P | P | P | P | P | P | T | P | P | P | | | | | | | | | | | | | | | | 0 | 0 |
| 70 | L | L | L | L | L | L | L | L | L | L | | | | | | | | | | | | | | | | 0 | 0 |
| 71 | S | S | S | S | S | S | S | S | S | S | | | | | | | | | | | | | | | | 0 | 0 |
| 73 | P | P | P | P | P | P | P | P | P | P | | | | | | | | | | | | | | | | 0 | 0 |
| 99 | P | P | P | P | P | P | P | P | P | P | | | | | | | | | | | | | | | | 0 | 0 |
| 100 | E | E | E | E | E | E | E | E | E | E | | | | | | | | | | | | | | | | 0 | 0 |
| 103 | H | H | H | H | H | H | H | E | D | H | H | | | | | | | | | | | | | | | 0 | 0 |
| 104 | F | F | F | F | H | H | H | Y | C | H | H | | | | | | | | | | | | | | | 0 | 0 |
| 106 | P | P | P | P | P | P | P | P | P | P | | | | | | | | | | | | | | | | 0 | 0 |
| IDs1 | RhoA | | | | | | | | | | | | | | | | | | | | | | | | | 26 | 14 |
| | RhoB | | | | | | | | | | | | | | | | | | | | | | | | | 9 | 9 |
| | RhoC | | | | | | | | | | | | | | | | | | | | | | | | | 13 | 11 |
| | RhoD | | | | | | | | | | | | | | | | | | | | | | | | | 7 | 7 |
| | Rac1 | | | | | | | | | | | | | | | | | | | | | | | | | 8 | 22 |
| | Rac2 | | | | | | | | | | | | | | | | | | | | | | | | | 17 | 7 |
| | Rac3 | | | | | | | | | | | | | | | | | | | | | | | | | 40 | 13 |
| | RhoG | | | | | | | | | | | | | | | | | | | | | | | | | 21 | 21 |
| | TC10 | | | | | | | | | | | | | | | | | | | | | | | | | 11 | 13 |
| | Rif | | | | | | | | | | | | | | | | | | | | | | | | | 9 | 9 |
| | Cdc42 | | | | | | | | | | | | | | | | | | | | | | | | | 20 | 32 |
| | | | | | | | | | | | | | | | | | | | | | | | | | | 16 | 8 |
| | | | | | | | | | | | | | | | | | | | | | | | | | | 8 | 14 |
| | | | | | | | | | | | | | | | | | | | | | | | | | | 7 | 7 |

Figure 2 Interaction matrix is launched to demonstrate interaction residues in all available structures. Left and upper parts comprise the amino acid sequence alignments of the RHO proteins and different GDIs, respectively. Each element corresponds to a possible interaction of RHO (row; Rac1 numbering) and GDIs (column; GDI1 numbering) residues. As indicated, interaction matrix represents three main regions, which cover the main interacting interfaces. Three main regions, comprising the main hotspot for the RHO-GDI interaction, are highlighted in the figure.

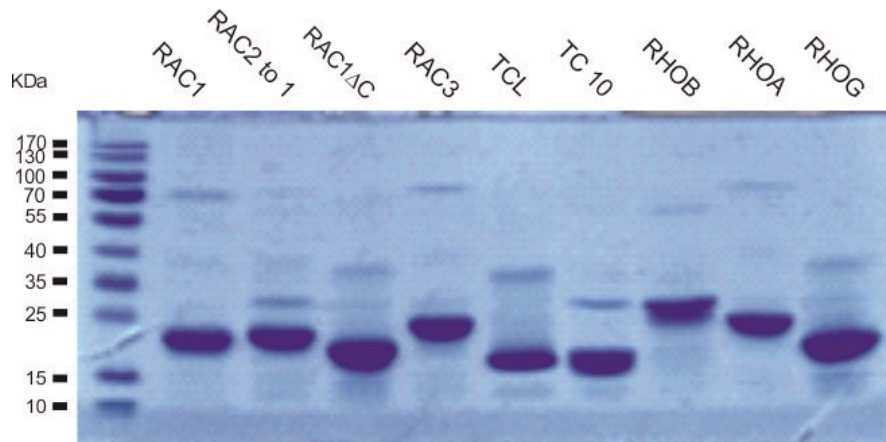


Figure 3 Coomassie dye gel of purified RHO proteins from *E. coli* expression system.

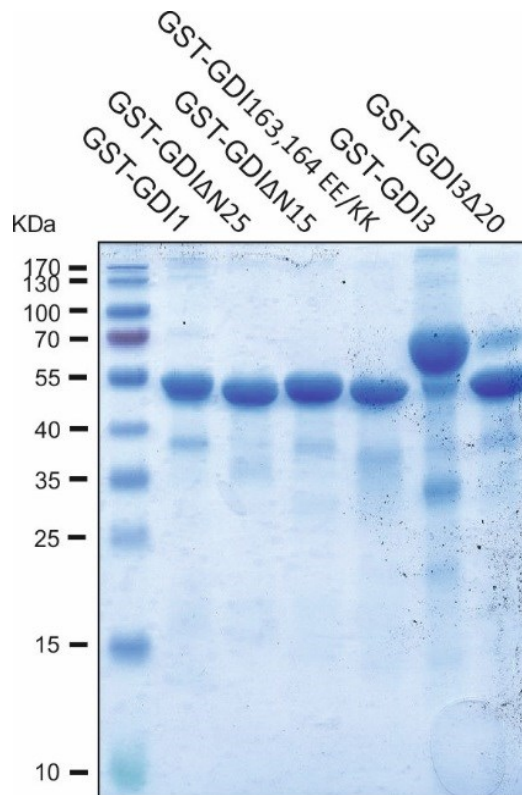


Figure 4 Coomassie gel of purified RHOGDI proteins from *E. coli* expression system. A truncated version of GDI3 was purified to stabilize it but the data showed no difference.

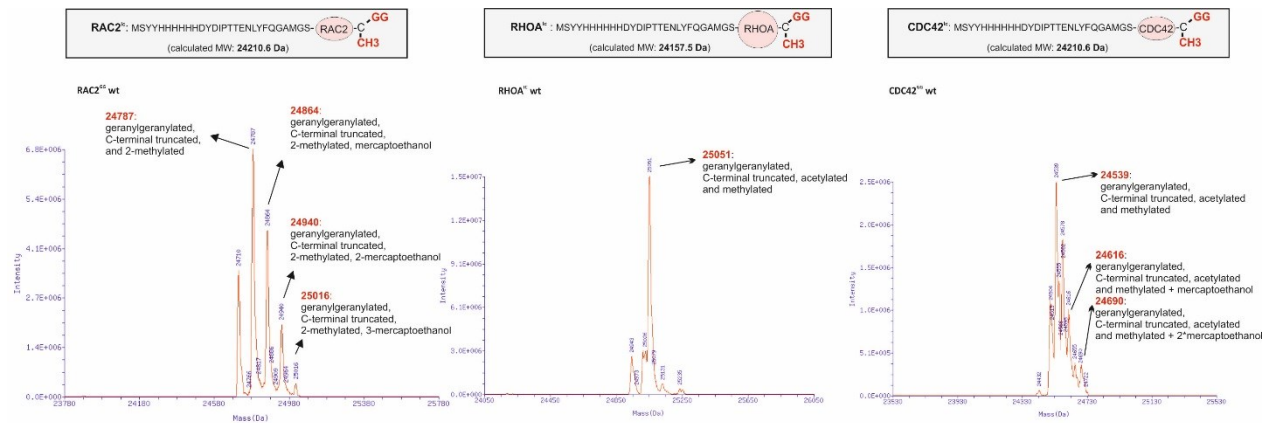


Figure 5 Mass spectrometry analysis of protein purified from insect cell system.

To gain insight into the mechanism of GDI function toward RHO proteins, kinetic and binding affinity of the interaction between RAC1^{GG} and non-prenylated RAC1 was analyzed. Using stopped flow and fluorescent-labelled mant-dGDP-RAC1, observed rate constant (k_{obs}) of interaction between RAC1 or RAC1^{GG} with GDI measured. It showed a difference of less than three-folds between prenylated and non-prenylated RAC1 (Fig. 7a). Surface plasmon resonance (SPR) measurement of the interaction between immobilized GST-GDI with increasing concentrations of RAC1^{GG} or RAC1 provides binding affinity (K_d) (Fig. 7b). Accordingly, there was not a huge difference between the binding affinity of prenylated RAC1 and GDI (SPR: K_d = 63 nM) compared to the non-prenylated RAC1 (SPR: K_d = 300 nM) (Fig. 7b). To proof this result, we used fluorescence polarization methods. In this case, labelled RAC1 was titrated by increasing concentrations of GDI. The measured affinity was in good agreement with SPR results and it showed K_d of 380 nM and 960 nM for prenylated and prenylated non-RAC1, respectively (Fig. 7c d). As a third proof, we used stopped-flow to measure the kinetic of interaction of GDI with fluorescent labelled-RAC1^{GG} and RAC1. Based on this method, we were able to measure k_{on} and k_{off} , for the rate of association and dissociation, respectively. k_{obs} value was measured by monitoring association of mant-dGDP RAC1 proteins with different concentrations of GDI1 (Fig. 7e-g). k_{obs} was fitted in a linear mode as a function of GDI concentrations and the slope of fitted line provides the k_{on} values (Fig. 7e). Displacement of GDI from fluorescently labeled RHO proteins measured by mixing the mant-dGDP RHO proteins in complex with the GDI1 with an excess amount of non-fluorescent GDP RHO proteins to obtain the k_{off} values (Fig. 7f). From the ratio of k_{off}/k_{on} we are able to calculate dissociation constant (K_d) (Fig. 7g). Obtained data proposed that non-prenylated RAC1 is able to bind GDI with a high affinity and it highlights the impact of protein-protein interface between the complex of RAC1 and GDI. Previously, it was reported that non-

prenylated RHOA is able to strongly associate with GDI, which proposed another function for GDI as a transporter of RHO to geranylgeranyl transferase enzyme on ER (Tnimov et al., 2014).

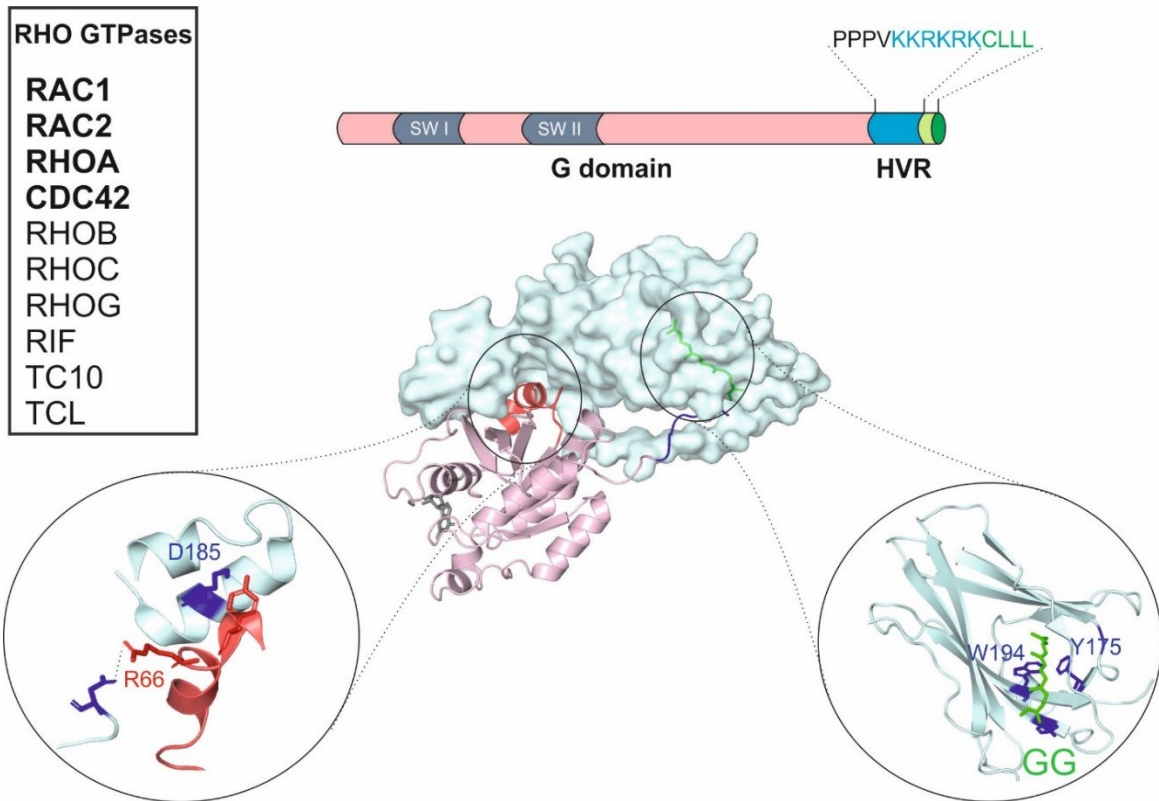


Figure 6 Crystal structure of GDI/RAC1 complex (PDB code: 1HH4). There are two main interfaces between GDI and RAC1 involving the interaction the geranylgeranyl moiety with W194 and Y 175 residues of GDI and Switch II region of RAC1 (mainly R66) with D185 from GDI. SW: switch region, HVR: hypervariable region.

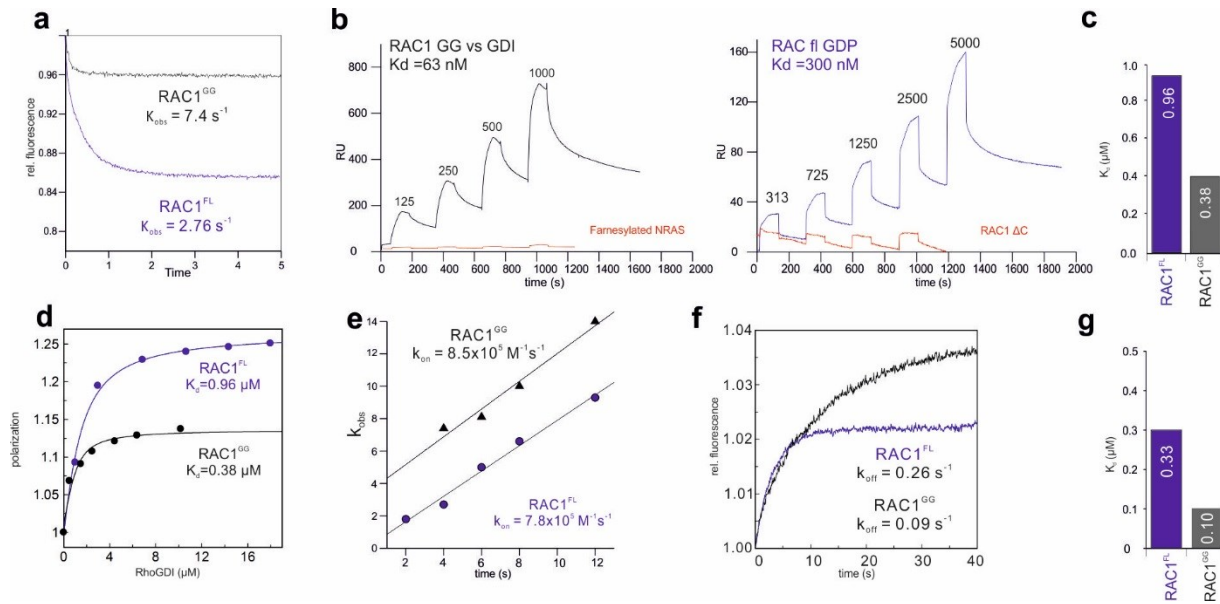


Figure 7 Non-prenylated RAC1 bound with high affinity to GDI a-g. SPR measurement of immobilized GST-GDI on anti-GST antibody coupled chip resulted in a 65 nM and 300 nM affinity for RAC1^{GG} and prenylated RAC1, respectively (a). The equilibrium mode using fluorescence polarization also showed a nanomolar affinity for both, prenylated and non-prenylated RAC1 (b, c). K_{obs} measurement of RAC1^{GG} and non-prenylated RAC1 showed three-fold difference (d). Quantitatively measurements of GDI1 interaction with RAC1^{GG} and non-prenylated RAC1 allowed us to calculate individual binding constants, including association rate constant or k_{on} (e), dissociation rate constant or k_{off} (f), and dissociation constant or K_d directly from the k_{off}/k_{on} ratio (g).

3.1.2. Liposomal reconstitution of RHO and GDI interaction

To analyze the function of GDI as a membrane cycling factor, we used liposome sedimentation assay as explained in detail in method part. Synthetic liposomes were generated using a defined amount of various lipids enriched by PI(4, 5)P₂ and PS, to have a biomimetic membrane. Briefly, a lipid mixture (500 μg), containing 10% (w/w) PE (in case of fluorescent liposome 5% (w/w) NBD-PE was also added), 45% (w/w) PC, 20% (w/w) PS, 10% (w/w) Cholesterol, and 5% (w/w) PIP₂. (Zhang et al., 2014). Prenylated RAC1 proteins bound to the synthetic liposomes and were pulled down by centrifugation (20000g for 20 min) and unbound proteins remain in supernatant (Fig. 8) Furthermore, addition of GDI1 and 2 led to displacement of liposome-bound RAC1^{GG}, RAC2^{GG}, RHOA^{GG}, CDC42^{GG}, which clearly indicates the function of GDI1 and 2 as a displacement factor

(Fig. 8). GDI3 did not function as displacement factor for RAC1, RAC2, CDC42 and RHOA. Based on the literature, GDI3 localized on the Golgi and mainly targets RHOB and RHOG (REF).

To understand the functional impact of geranylgeranyl moiety interaction with GDI (It refers to RHOGDI1), we used its analogue, geranylgeranyl pyrophosphate (GGpp), to inhibit the hydrophobic pocket of GDI and avoid the insertion of this geranylgeranyl moiety of RHO proteins (Fig. 9). Excess amount of GGpp was incubated with GDI and liposome sedimentation was performed to analyze GDI potential as a liposome displacement factor. Quantified western blot data indicates that GGpp does not obviously inhibit GDI function. This data suggests that geranylgeranyl moiety does not play a crucial role in GDI complex formation and there are other central interfaces (Fig. 9).

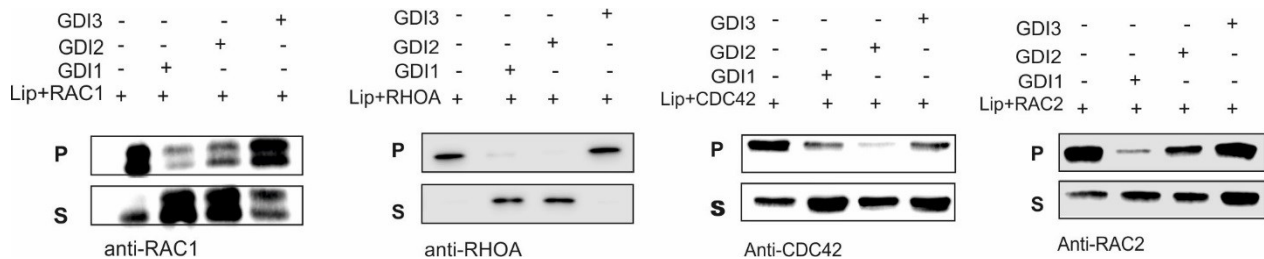


Figure 8 Displacement of liposome-bound prenylated RHO proteins by GDI1, 2 and 3. Synthetic liposome containing PIP₂ were mixed with prenylated RHO proteins and centrifuged after incubation for 20 min. Pellet and supernatant samples were prepared for western blotting. Obtained results showed that GDI1 and 2 displaced RHO proteins from liposome but GDI3 could not function as displacement factor.

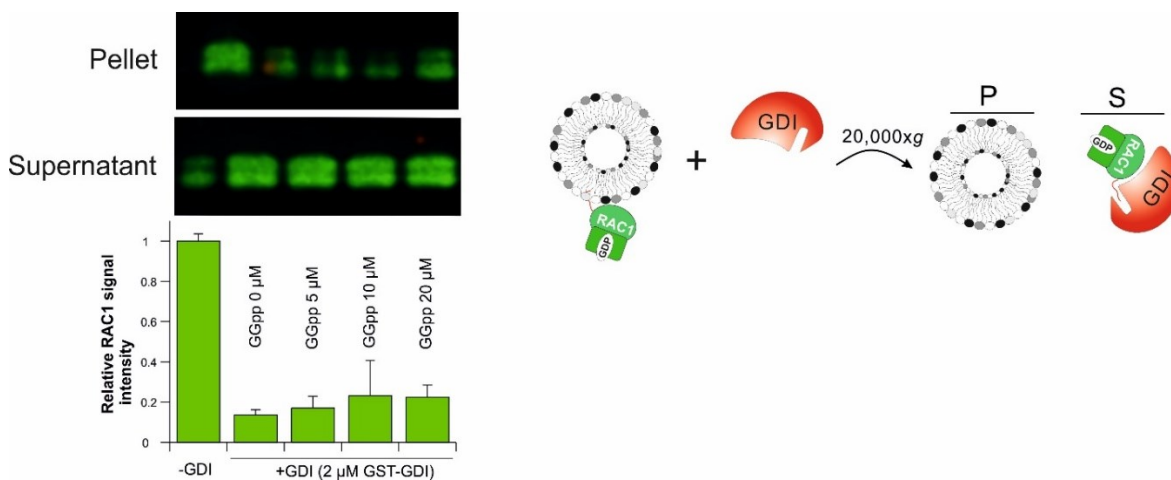


Figure 9 Geranylgeranyl pyrophosphate (GGpp) does not inhibit GDI function over RAC1^{GG}. RAC1^{GG} binds to the synthetic liposome and pulled down as pellet by centrifugation. Displaced RAC1^{GG} by GDI, appeared in supernatant. Molar excess of GGpp does not inhibit the function of GDI. The right panel shows the scheme of experiment procedure in which GDI displaces RAC1^{GG} from liposomes.

RHO proteins contain three distinct regions: G-domain, which is conserved between RHOs and involves switch I/II parts. Hypervariable region (HVR), which makes the differences between RHOs and involves polybasic motifs, and at the very C-terminus of RHO protein sequence exists a CAAX box, which is the target of prenylation and remains conserved within RHOs (Fig. 6) (Moon, 2003). To understand the binding behavior of different RHO proteins toward GDI, observed rate constant of RHOs interaction with GDI monitored (Fig. 10). Obtained data showed a variable pattern in which RAC1, RAC3 and RHOA indicated the highest values compared to the others (Fig. 11). RAC2, RAC1^{ΔC} and CDC42 did not show any association (Fig. 11). This variable pattern could not be explained with G-domain as central interface because it is conserved within different RHO proteins (Fig. 2). Then, we proposed that HVR is involved in complex formation, which has a different pattern of residues between RHO family members. Moreover, RAC1, RAC3 and RHOA contain an enrich polybasic sequence in their HVR compared to other RHOs like CDC42 and RAC2. Here, we expected an electrostatic interaction network which leads to a higher value of k_{obs} for RAC1 but not RAC2.

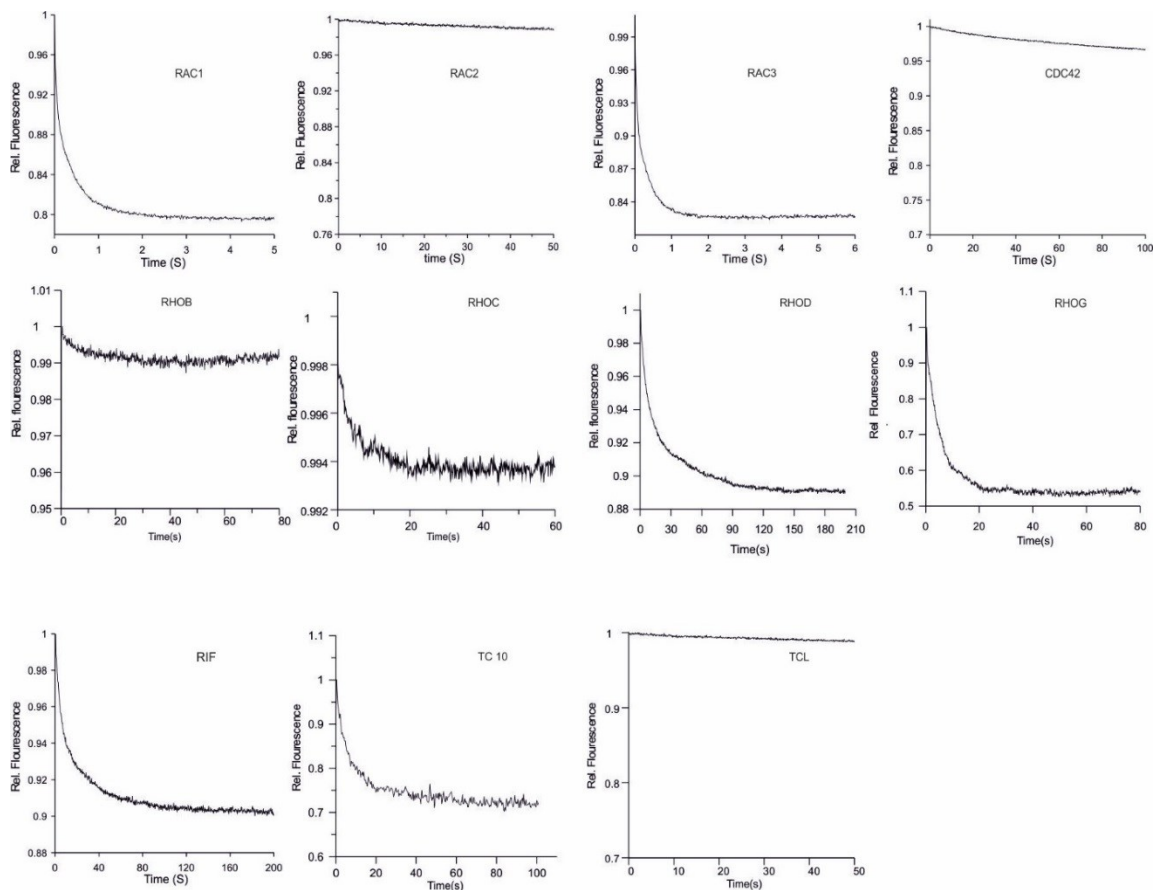


Figure 10 k_{obs} monitoring of interaction between fluorescent-labelled RHO proteins and GDI1 using stopped-flow measurement.

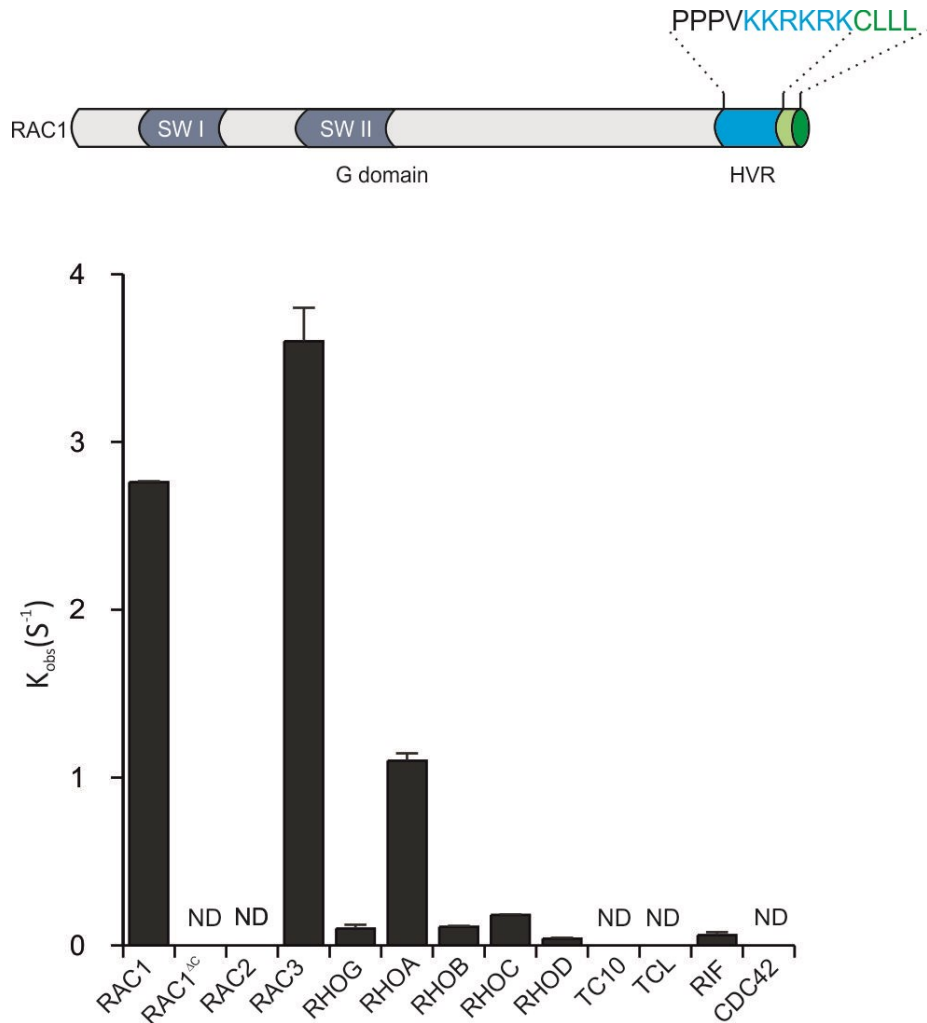


Figure 11 K_{obs} measurement of different prenylated, mant-dGDP-bound RHO GTPase toward GDI1 using stopped flow. The measurements indicate that RAC1^{FL} and RAC3^{FL} rapidly associated with GDI1, and also RHOA^{FL}, but not RAC2^{FL} and CDC42A^{FL}. ND: Not detected, SW: switch, HVR: hypervariable region.

To analyze the impact of HVR in this interaction study, we study the HVR interface with GDI. Crystal structure of RAC1 and GDI indicates an interface between polybasic residues (blue) and negatively charged cavity in GDI (red) (Fig. 12a). Based on this information, various mutation performed in HVR of RAC1 and RAC2 in order to understand the impact of positively charged residues in binding affinity. We made mutations in three position in the HVR of RAC2 (+3) to generate the same net positive charges as exist in RAC1 (+6). Another generated construct contains reverse mutations of five positive charges to five negative charges (KKRKRK/EEEE) (Fig. 12a). RAC1 delta C (ΔC) also used as negative control. Further kinetic and affinity measurements indicated that mutations in the HVR of RAC2 to RAC1 (RAC2^{QQKRA/KKKRK}) led to association (Fig. 12b). Moreover, K_d measurement indicated that positively charged residues are proportionally

involved in the affinity of binding. RAC1 bound with 300 nM affinity to GDI while RAC2 has an affinity of 1.1 μ M. RAC2^{QKRA/KKKRK} construct showed high affinity in the range of RAC1, which perfectly supports the impact of positive charges in the HVR of RHO proteins (Fig. 13a, b). Furthermore, RAC1^{KRKRK/EEEE} showed a drastic decrease of ten-fold in K_d (Table 3).

To prove the interface between polybasic region of RAC1 and negative cavity of GDI, GDI was mutated in the position of 163 and 164 (EE to KK). Crystal structure analysis indicated that residues E163 is involved in a hydrogen binding network formed by K188 of RAC1 (Fig. 12a). We made a construct by mutating 163,164EE/KK to see the impact of this region. The residues of 164E was also mutated to avoid its compensation impact for E163. Additionally, flexible N-terminal region of GDI contains two negatively charged areas, which could be involved in this electrostatic network. Previous study also showed the significance of the first 25 residues of GDI in its function as a displacement factor (Ueyama et al., 2013). Then, GDI ^{Δ N25} was generated to analyze the impact of this region as well. GDI ^{Δ N15} was also generated and investigated, to show that the negative-rich region of 19-22aa is important for GDI function not the negative charges in residues 1-15aa (Fig. 12a). Liposome sedimentation assay performed to analyze the impact of negatively charged cavity (red) and N-terminal hand (yellow) of GDI in its function (Fig. 12a). Prenylated RAC1^{GDP} added to the liposomes suspended in protein buffer (20 mM HEPES, pH 7.4, 50 mM NaCl, 3 mM DTT) and incubated for 20 min on ice (Fig. 14). Next, GDI was added to the sample and further incubated on ice for 30 min. Next, the samples were centrifuged at 20000g for 20 min at 4 °C. The obtained pellet and supernatant fractions were collected and analyzed by western blotting (Fig. 14). Data showed that GDI with deletion of its first 25 could not displace RAC1 from liposomes but it binds to the liposome fraction (pellet). Moreover, mutation of E163 could not function as RAC1 displacement factor and it behaves like GDI ^{Δ N25} (Fig. 14). It shown that GDI ^{Δ N15} which has a normal function. Western blot analysis of pellet fraction with anti-GST antibody indicates that GDI ^{Δ N25} and GDI^{163,164EE/KK} are in liposome fraction which means these constructs are able to bind RAC1 but could not displace it from liposome (Fig. 14).

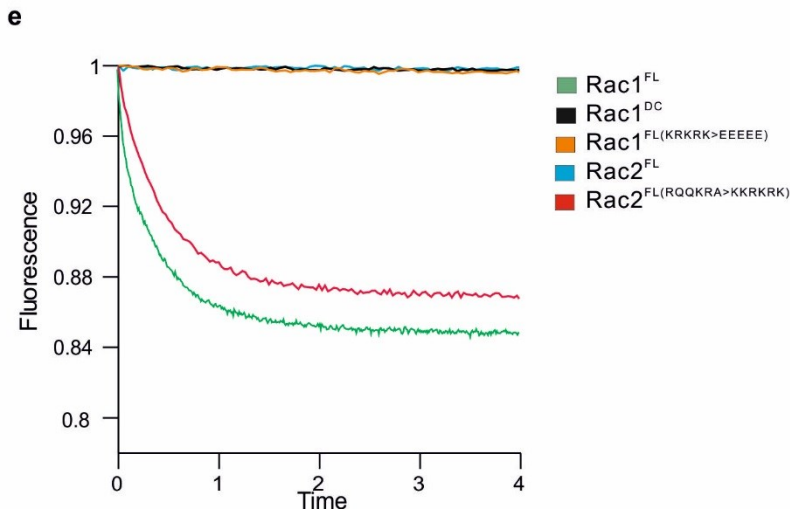
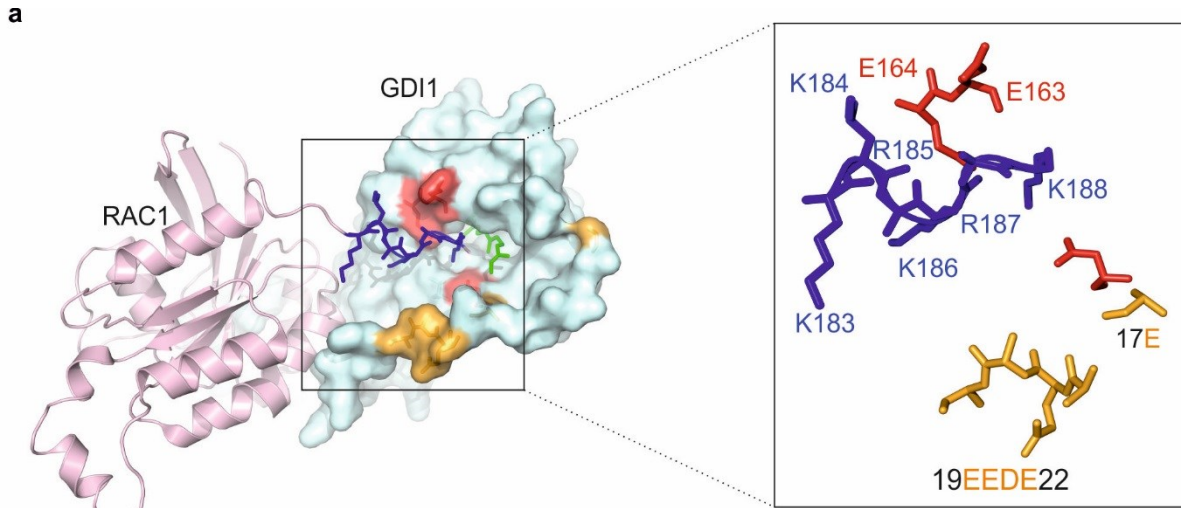


Figure 12 Polybasic residues contribute to GDI binding. The structure of GDP-bound RAC1^{GG} (ribbon) in complex with GDI1 (surface) highlights various GDI segments and the basic HRV (blue) sandwiched between acidic residues (red) and N-terminal region (yellow) of GDI (a). Sequence alignment of the RHO HVRs showed significant differences in the frequency of the basic residues (a). Lack of a RAC2 wild-type association with GDI1 was rescued by its mutation at the C-terminus to RAC1 (RQQKRA to KKRKRK). Deletion of RAC1 HRV or its mutation (KRKRK to EEEEE) completely abolished GDI association with RAC1 (b).

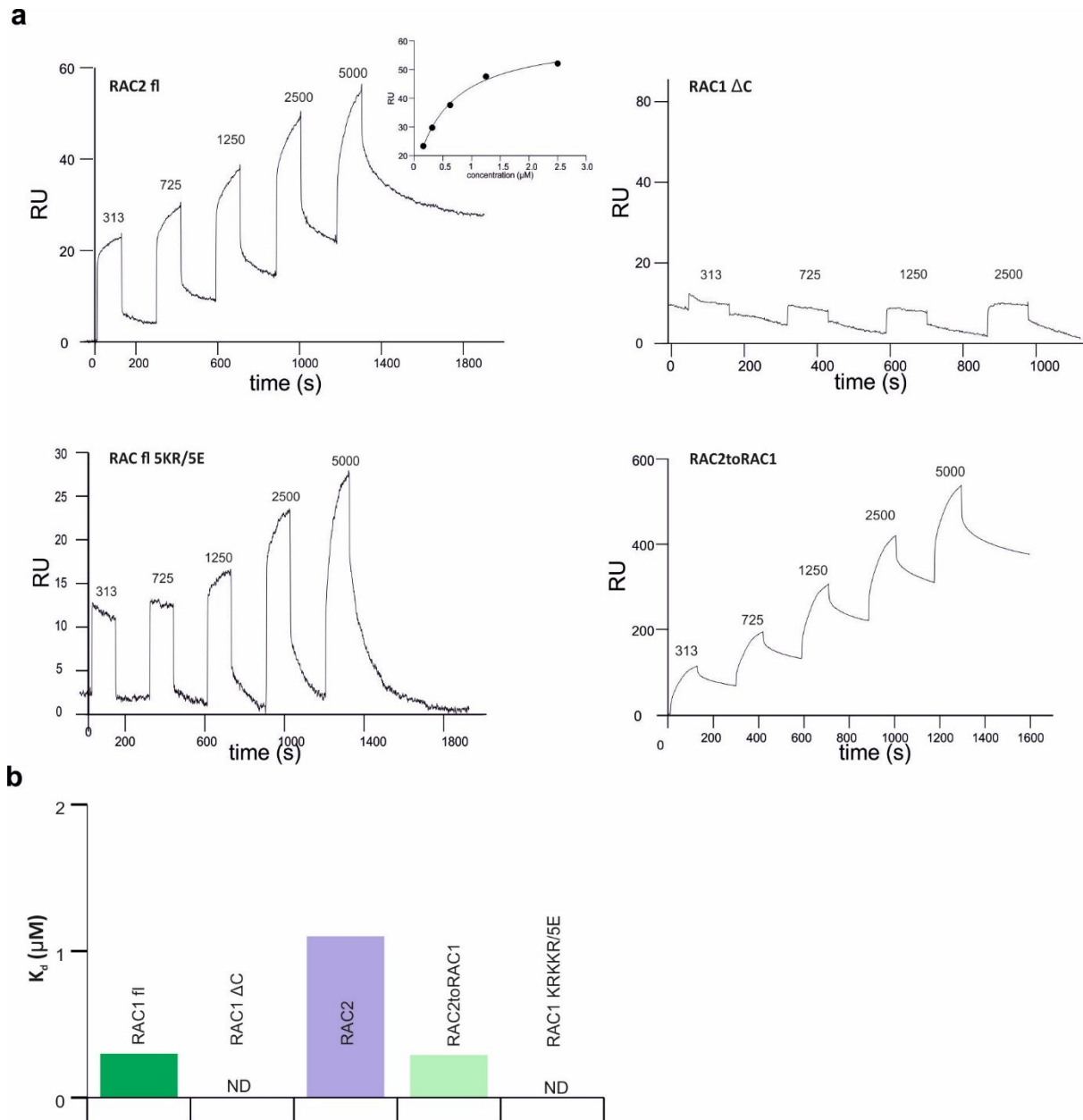


Figure 13 Polybasic residues in HVR contribute to high affinity binding. K_d (dissociation constant) values, obtained by SPR measurement revealed that RAC1^{FL} binds GDI1 more than 3 and 10-fold tighter than Cdc42A^{FL} or RAC2^{FL}, respectively. RAC2^{RQQKRA<KKRKRK} (RAC2toRAC1) mutant binds to GDI with the high affinity likes RAC1^{FL}.

Table 3 Direct binding of RHOGDI vs RHO proteins using antibody-GST chip coupled with GST-GDI.

| Immobilized GST-GDI | K_a (1/M.sec) | SE (k_{on}) | K_{off} (1/sec) | SE (k_{off}) | K_d (M) |
|--------------------------|-------------------|------------------|----------------------|------------------|----------------------|
| RAC1 ^{GDP} | $1.9 \cdot 10^3$ | 83 | $6.1 \cdot 10^{-4}$ | 56 | $3.0 \cdot 10^{-7}$ |
| RAC1 ^{GppNHp} | $1.3 \cdot 10^3$ | 65 | $5.4 \cdot 10^{-4}$ | 52 | $4 \cdot 10^{-7}$ |
| RAC2 | - | - | - | - | $1.1 \cdot 10^{-6}$ |
| RAC1 ^{ΔC} | - | - | - | - | - |
| RAC1 ^{KRKKR/5E} | 62 | 9.1 | $1.7 \cdot 10^{-4}$ | 50 | $2.8 \cdot 10^{-4}$ |
| RAC2toRAC1 | $3 \cdot 10^3$ | $1.5 \cdot 10^2$ | $9.0 \cdot 10^{-4}$ | 54 | $2.9 \cdot 10^{-7}$ |
| RAC1 ^{GG} | $1.36 \cdot 10^4$ | 57 | $8.59 \cdot 10^{-4}$ | 46 | $6.3 \cdot 10^{-8}$ |
| RHOA ^{GG} | $1.0 \cdot 10^3$ | 14 | $5.57 \cdot 10^{-4}$ | 37 | $5.38 \cdot 10^{-7}$ |
| RAC2 ^{GG} | $4.8 \cdot 10^4$ | 78 | $1.0 \cdot 10^{-3}$ | 60 | $2.1 \cdot 10^{-7}$ |
| CDC42 ^{GG} | $1.5 \cdot 10^3$ | 7.8 | $3.5 \cdot 10^{-4}$ | 21 | $2.3 \cdot 10^{-7}$ |

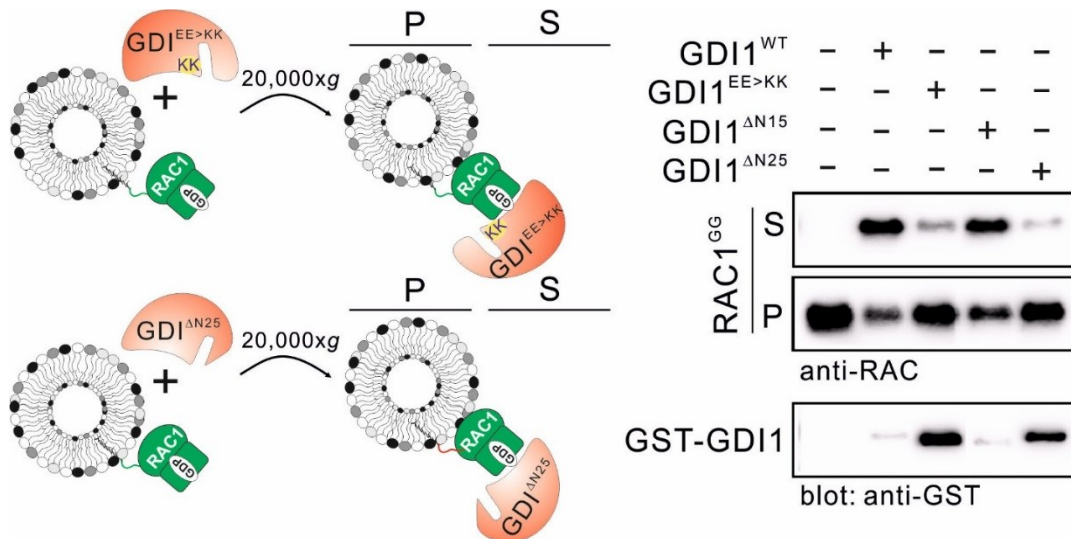


Figure 14 Liposome sedimentation of RAC1^{GG} in the presence of various GDI mutants. Substitution of E163 and E164 for lysine or deletion of the N-terminal 25 amino acids ($\Delta N25$) but not $\Delta N15$ disabled GDI1 in displacing RAC1 from the liposomes although these GDI1 variants remained in the complex with RAC1 on the liposomes (h).

3.1.3. Kinetic analysis of RHO membrane cycling

RHO GTPases are lipidated, which targets them to the membrane. Moreover, HVR of various RHO GTPases is enriched by positively charged residues, which contributes to an electrostatic interface (Fig. 11). Previous studies have shown that not only prenylation but also this polybasic region are needed for efficient membrane binding of GTPases. Then, GDI needs to compete with these membrane-binding interfaces (Jang et al., 2015; Michaelson et al., 2001).

Biacore X100 instrument (GE Healthcare) used to analyze RHO protein interaction toward GDI1 in the presence of synthetic membrane. Liposomes were immobilized by injecting 500 μM liposomes (5 $\mu\text{L}/\text{min}$) in buffer (20 mM HEPES, 150 mM NaCl, 5 mM MgCl_2 , 3 mM DTT at pH 7.4) on the surface of a L1 sensor chip (GE Healthcare) for the period of 900 s. The unbound liposomes were removed by passing the buffer containing 10 mM NaOH (5 $\mu\text{L}/\text{min}$ for 30 S) over sensor chip. Next, 15 μM prenylated RAC1^{GG} was injected (5 $\mu\text{L}/\text{min}$) over the immobilized liposomes and the liposome association was monitored based on the mass transport to the surface (Fig. 15). Afterward, buffer flow to the system and the dissociation of RAC1 from liposome monitored. As control, C-truncated RAC1 was injected to the system and it showed no significance liposome interaction compared to RAC1^{GG}. Next, GDI1 (25 μM) was injected to the system which led to mass subtraction from the surface of the chip due to the displacement of RAC1 from immobilized lipids (Fig. 15). Addition of GDI to the immobilized RAC1^{GG} led to the decrease of signal due to the displacement of proteins from the immobilized liposomes over the surface of the chip and non-linear fitting of the graph gave us k_{off} of the RAC1^{GG} displacement by GDI (Fig. 15). Fitted curve shows the dissociation rate constant of 0.014 s^{-1} (Fig. 15). This optimized SPR framework provides us the ability to monitor and analyze the membrane cycling of various RHO proteins.

To analyze the impact of geranylgeranyl moiety and HVR in membrane cycling of RHO proteins, liposome cycling of prenylated RHO proteins was analyzed by SPR (Fig. 16). Increasing concentrations of RHO proteins injected to the immobilized liposomes and kinetics parameter obtained by fitting the final curves to a one: one kinetic mode. Obtained data showed that prenylated RAC1 binds 10-fold stronger than non-prenylated one (Table 4). Comparing the on and off rate indicates that the main difference is the dissociation rate of RAC1^{GG} which is ten-fold slower than non-prenylated RAC1 (Table 4). Nucleotide dependent binding also indicates that RAC1^{GDP} has three-fold higher affinity than the RAC1^{GppNHp} form, which is mainly due to the contribution of higher association rate up to six-fold (Table 4).

Kinetic analysis of membrane cycling of other prenylated RHO proteins indicated that RAC2^{GG} had very low affinity toward membrane while CDC42^{GG} showed the affinity of 40 nM (Table 4). CDC42 has negative charges in its HVR, which could contribute in electrostatic interaction with positively charged PE lipids. RHOA^{GG} has also an affinity of 380 nM and ten-fold lower association rate than RAC1 because of lower electrostatic potential in its HVR. In fact, membrane cycling of prenylated RHO proteins are mainly influenced with differences in association rates.

Table 4 Kinetic parameter of RHO GTPase membrane cycling.

| Immobilized Liposome | K _a (1/M.sec) | SE (k _{on}) | K _{off} (1/sec) | SE (k _{off}) | K _d (M) |
|------------------------|--------------------------|-----------------------|--------------------------|------------------------|----------------------|
| RAC1 ^{GDP} | 6.5*10 ⁺³ | 77 | 2.2*10 ⁻³ | 65 | 3.4*10 ⁻⁷ |
| RAC1 ^{GppNHp} | 0.9*10 ⁺³ | 26 | 9.8*10 ⁻³ | 4.1*10 ⁻⁵ | 1.0*10 ⁻⁶ |
| RAC1 ^{GG} | 1.0*10 ⁺⁴ | 41 | 3.4*10 ⁻⁴ | 20 | 3.3*10 ⁻⁸ |
| RHOA ^{GG} | 1.1*10 ⁺³ | 17 | 4.25*10 ⁻⁴ | 7.7 | 3.8*10 ⁻⁷ |
| RAC2 ^{GG} | 4.2*10 ⁺³ | 21 | 5.8*10 ⁻³ | 35 | 1.3*10 ⁻⁶ |
| CDC42 ^{GG} | 1.3*10 ⁺⁴ | 1.3*10 ⁺² | 5.5*10 ⁻⁴ | 33 | 4.0*10 ⁻⁸ |

To understand whether GDI has a selective function in cell free condition, two and later three different RHO proteins (RHOA, RAC1 and CDC42) with the same molarity (1 μM from each) were incubated with synthetic liposomes. Liposome sedimentation assay performed and the pellet and supernatant fractions were analyzed by western blotting using anti-His antibody (all prenylated proteins are His-tag). In another condition, limited concentration of GST-GDI (1 μM) was added to the membrane bound RHO^{GG} proteins (3 μM in total), and function of GDI as liposome displacement factor was analyzed. GDI bound RHO proteins with a one-by-one stoichiometry and in a limited condition (molar ratio of GDI/RHO = 0.33) it could not bound at any given time to all RHO proteins. In this case, it is possible to analyze if GDI has preference in function toward various RHO proteins or not. After performing liposome sedimentation assay, western botting was performed using specific validated antibody (data not shown). To our supprise, GDI displaced completely CDC42^{GG} from membrane but not RAC1^{GG} and RHOA^{GG} (Fig. 17). To find out the reason of GDI preferences toward CDC42, affinity of GDI interaction to the individual RHO^{GG} protein was measured (Fig. 18) and was divided to the affinity of the same RHO^{GG} protein to the

synthetic liposome. Measured values indicated that CDC42 has three-fold higher ratio toward GDI compared with RAC1 and CDC42 (Fig. 19). Higher values mean that RHO proteins has higher affinity toward GDI than liposome. In fact, CDC42 prefers to remain in GDI bound form than associating with liposome. On the other hand, RHOA and RAC1 are strongly bound to the membrane and their displacement need a stronger interaction with GDI. Our study indicates that RHO proteins bind with two main regions of polybasic and geranylgeranyl moiety to the negatively charged membrane. GDI interacts with membrane bound RHO proteins and displacement them by interfering with polybasic region interface and membrane. In the light of above mentioned, HVR play a crucial role in this membrane cycling of RHO GTPases and GDI follows different kinetics for displacement of RHO proteins with an individual pattern of polybasic residues.

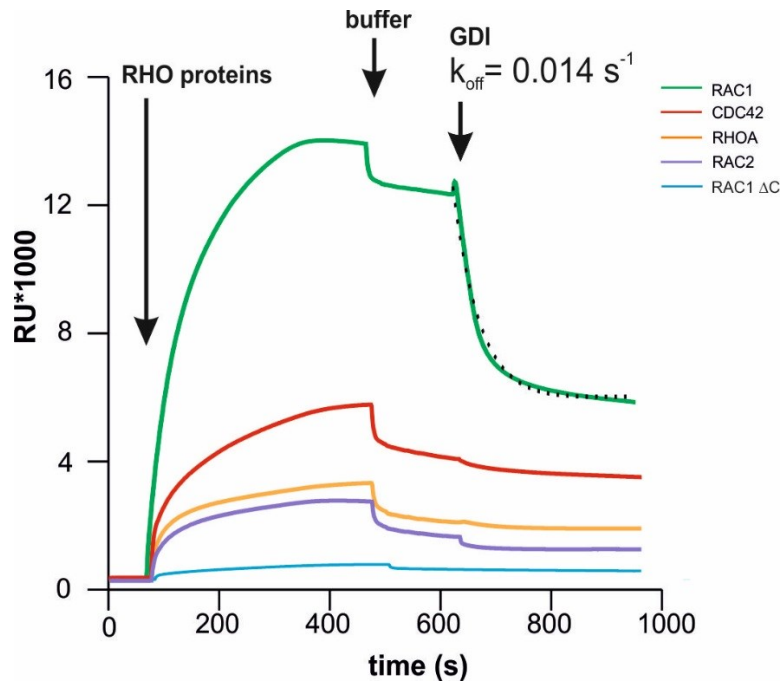


Figure 15 Displacement of liposome-bound prenylated RHO by GDI. RAC1 displacement by GDI was measured and fitted with non-linear fitting model (dot) to obtain the k_{off} of RAC1^{GG} membrane displacement.

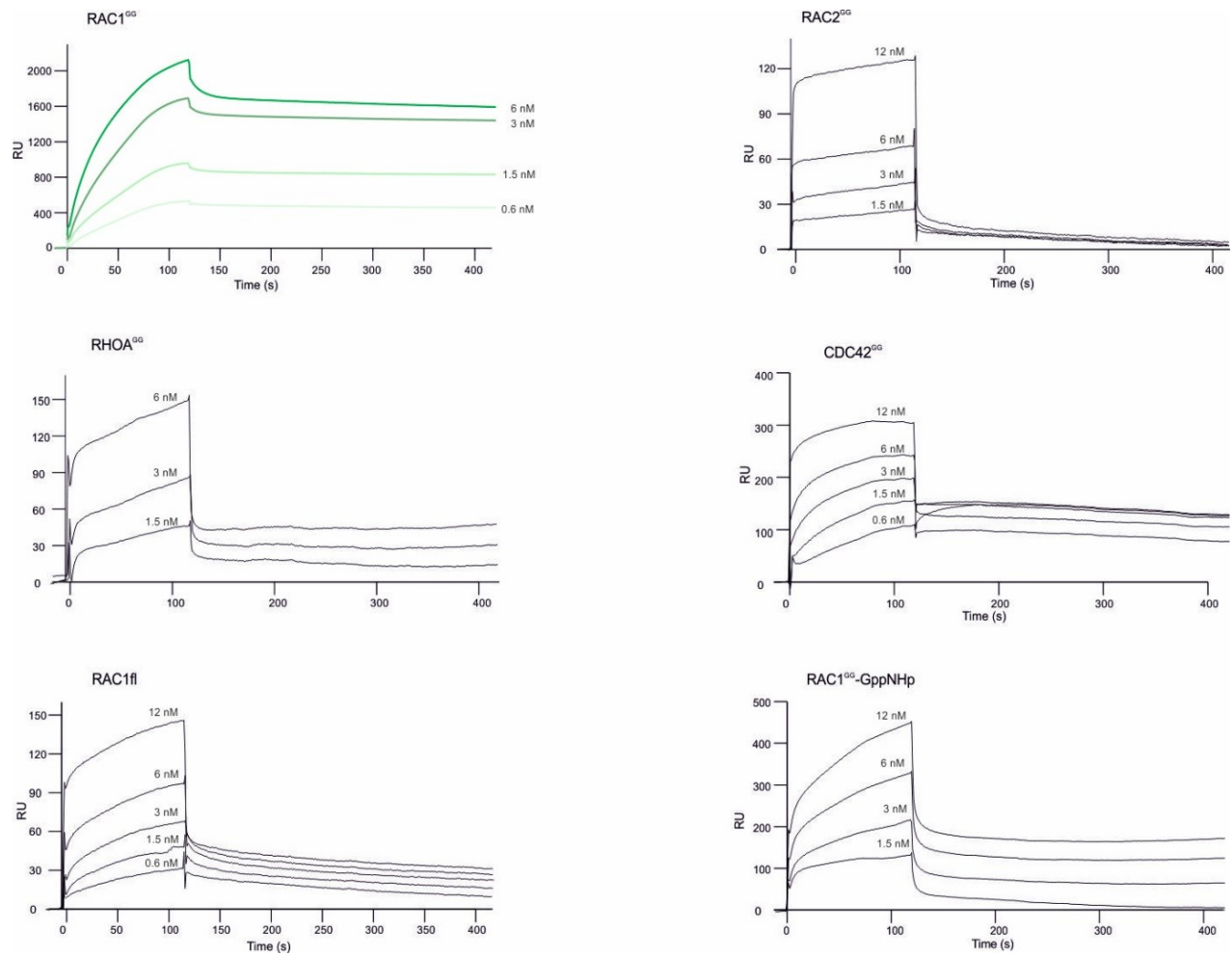


Figure 16 Liposome cycling of RAC mutant's was analyzed with SPR measurement. Different concentrations of RAC1 proteins were titrated to the immobilized liposome over a L1 chip, and dissociation of proteins monitored by addition of buffer. Dissociation curve was fitted to a non-linear mode to measure k_{off} . Nucleotide dependent membrane cycling of RAC1 was also analyzed using GDP and GppNHp forms of protein, which shows a 10-fold lower affinity for RAC1^{GppNHp} in comparison with RAC1^{GDP}.

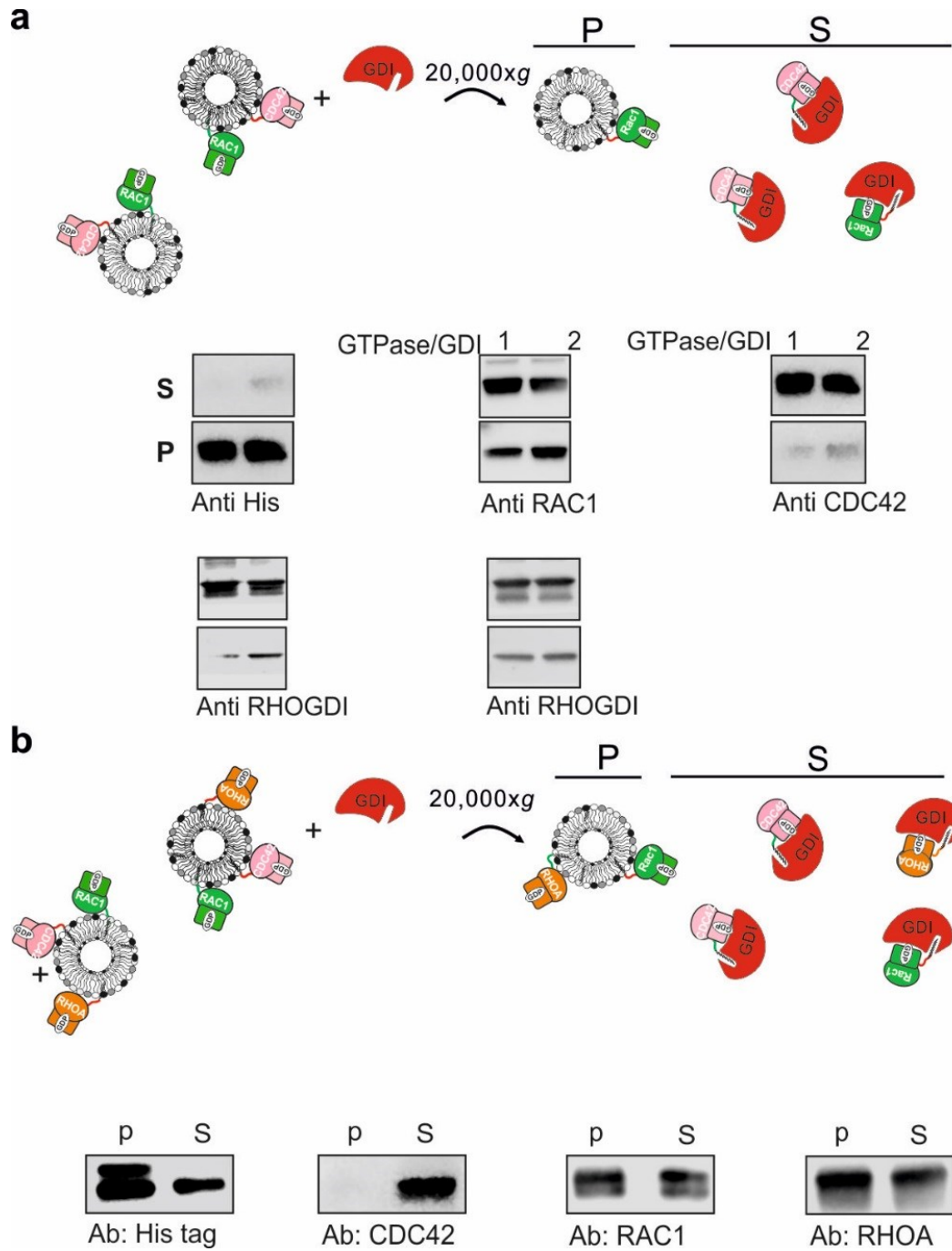


Figure 17 GDI selectively displaced CDC42 from liposomes. Comparable analysis of the GDI displacement function in limited concentration (1 μ M) and presence of two different RHO GTPases (1 μ M RAC1 and 1 μ M CDC42) revealed that GDI1 prefers to displace CDC42 (a). Competition analysis of GDI (1 μ M) function over three GTPases involving RAC1, CDC42 and RHOA (1 μ M from each) indicated a selective displacement of CDC42 as well (b).

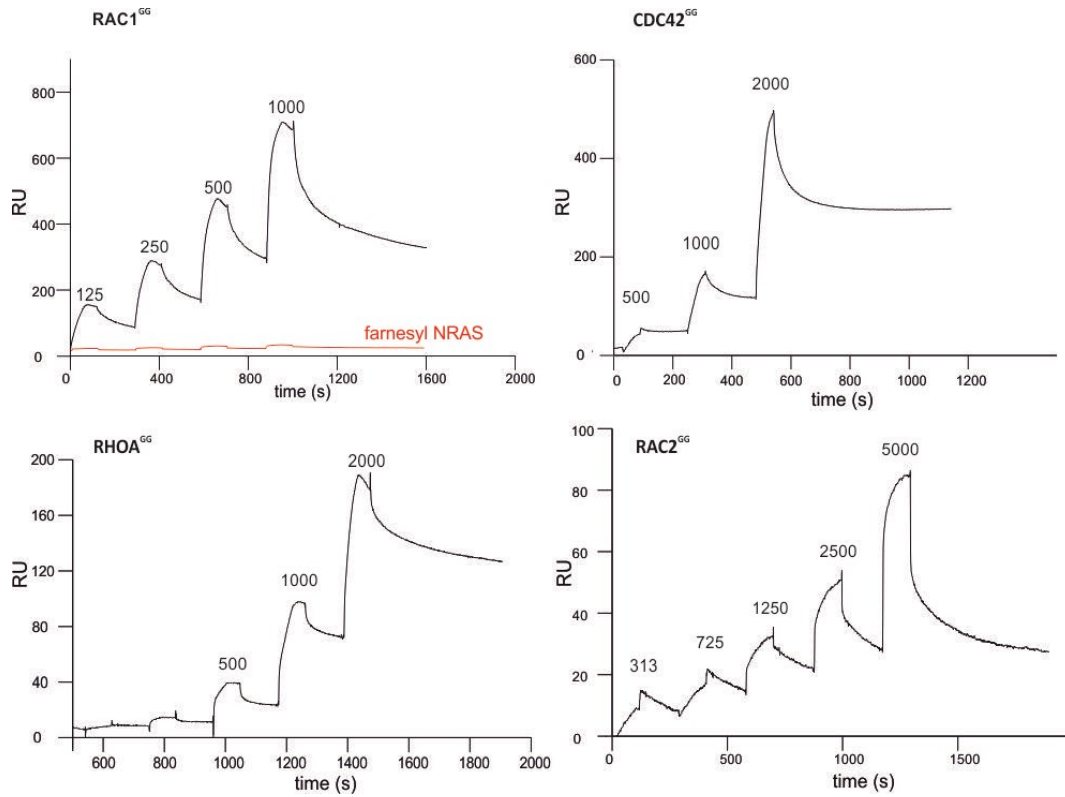


Figure 18 GDI binding of prenylated RHO GTPases. Prenylated RHO proteins were titrated to the surface of a GST-GDI immobilized CM5 chip in SPR. Obtained data are sorted in table 3.

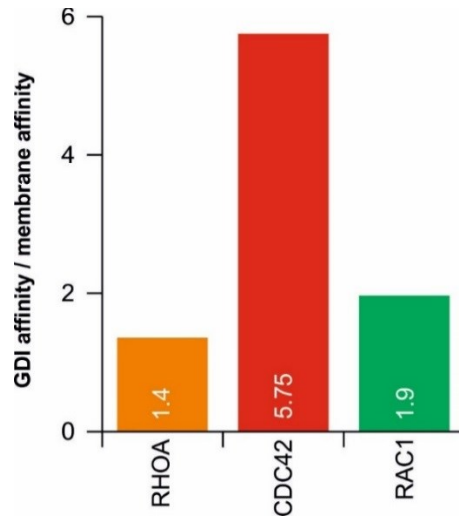


Figure 19 Affinity ratio of interaction of various RHO^{GG} with GDI/membrane. Obtained affinity of GDI interaction to prenylated RHO proteins (Table 3) were divided to the affinity of prenylated RHO to the liposomes (Table 4).

3.2. Chapter II: GDI in disease

3.2.1. CDC42 new mutant (R186C) found in patients showed GDI binding deficiency

CDC42 is another member of the RHO subfamily of GTPases is also cycling between a GTP-bound (active) and GDP-bound (inactive) states. Three different regulator families also regulate CDC42, involve the guanine nucleotide exchange factors (GEFs), GTPase-activating proteins (GAPs) and guanine nucleotide dissociation inhibitors (GDIs) (Nalbant et al., 2004; Smith et al., 2002). CDC42 controlling a wide ranges of cellular processes through interaction with various effectors (Baschieri et al., 2014; Zhou et al., 2013). CDC42 needs posttranslational modifications including prenylation at Cys¹⁸⁸ in CAAX (geranylgeranylation) followed by C-terminal processing (Aicart-Ramos et al., 2011). Mass spectrometry analysis on the immunoprecipitated disease-associated CDC42 mutant revealed proper lipid incorporation and C-terminal processing (data not shown), ruling out aberrant post-translational processing of CDC42 as a driver of pathogenesis. Arg¹⁸⁶ is positioned in the HVR and is out of the GDP/GTP binding pocket, which is the major region of RHO proteins for interaction with positive and negative regulators (Switches I and II) (Hemsath et al., 2005). Consistently, kinetic and binding affinity measurement assays showed the replacement of Arg¹⁸⁶ by a cysteine did not change the GEF dependent nucleotide exchange rate and GAP catalyzing GTP hydrolysis (data not shown). On the other hand, Arg¹⁸⁶ contributes to the intermolecular binding pocket stabilizing CDC42 binding to RHOGDI, which negatively controls translocation of the GTPase to the cytoplasmic leaflet of membranes, and modulates CDC42 trafficking (Gibson et al., 2004; Gibson and Wilson-Delfosse, 2001; Hoffman et al., 2000).

CDC42^{WT} and CDC42^{R186C} mutant were purified from insect cell system and analyzed protein posttranslational modifications using mass spectrometry. The data showed that both proteins receive the same modification by addition of GG moiety at the very C-terminal cysteine (Fig. 20). GST-GDI pull down assay was performed to analyze GDI binding ability of CDC42 constructs. GST-GDI was incubated with GST-beads and later CDC42 WT and mutant were added and incubated for 1 hour. After centrifugation and sample preparation, co precipitation of GDI and CDC42 was analyzed by western blotting. To our surprise, CDC42^{R186C} did not bind GDI while wild type protein was able to bind. Further analysis with liposome sedimentation assay, also showed the reduced displacement of CDC42^{R186C} from liposome (Fig. 21). Kinetic measurement of CDC42

interaction toward immobilized GST-GDI, clearly showed that CDC42 mutant did not bind GDI while wild type protein showed binding (Fig. 22).

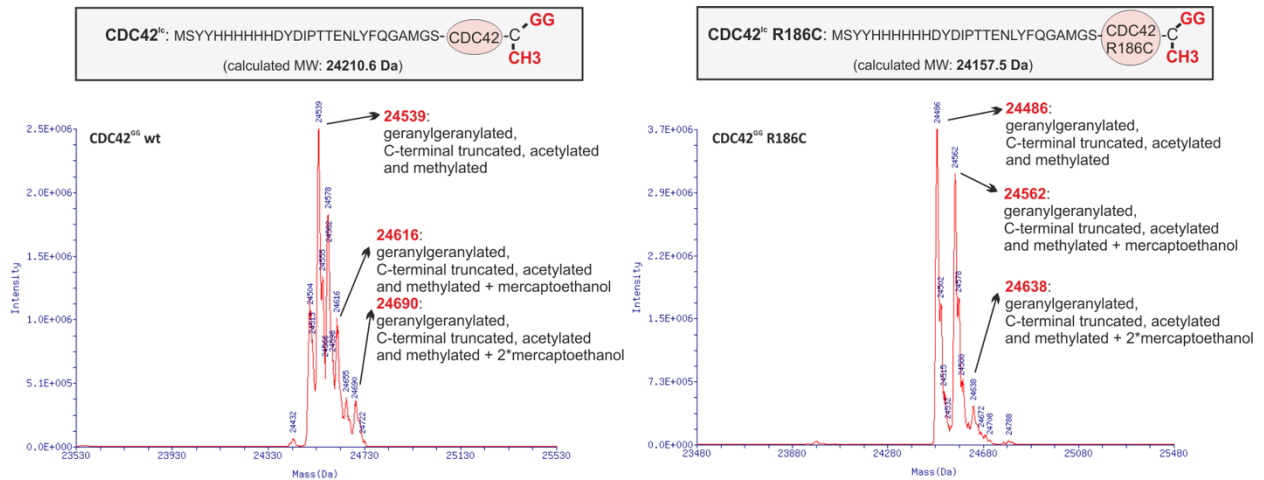
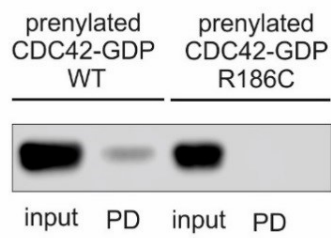


Figure 20 Mass spectra analysis of CDC42^{lc} wild type and R186C mutant showed a strong peak in 24539 and 24486, respectively. It indicates that CDC42^{WT} and mutant undergo the same posttranslational modification including geranylgeranylation followed by C-terminal modification. The additions of mercaptoethanol in both spectra generated two more variants.

a

PD: GST-GDI1
 WB: anti-CDC42

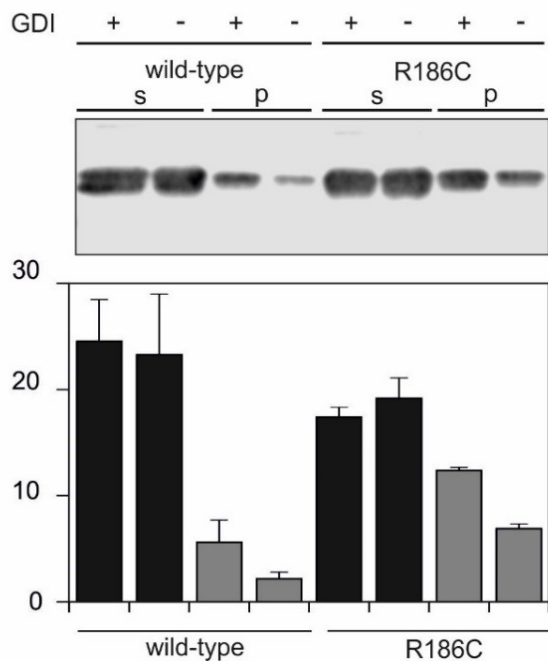
b

Figure 21 *In vitro* analysis of GDI function over wild type CDC42 and CDC42 R186C. a, GST-GDI pull down assay of CDC42 wild type and CDC42 mutant. GST-GDI could bind CDC42 wild type but not the mutant. b, Liposome pull down assay was performed using synthetic liposome and prenylated CDC42 wild type and R186C mutant. CDC42^{R186C} has higher membrane affinity but lower GDI binding potential. In fact, CDC42^{R186C} could not bind as efficient as CDC42 wild type.

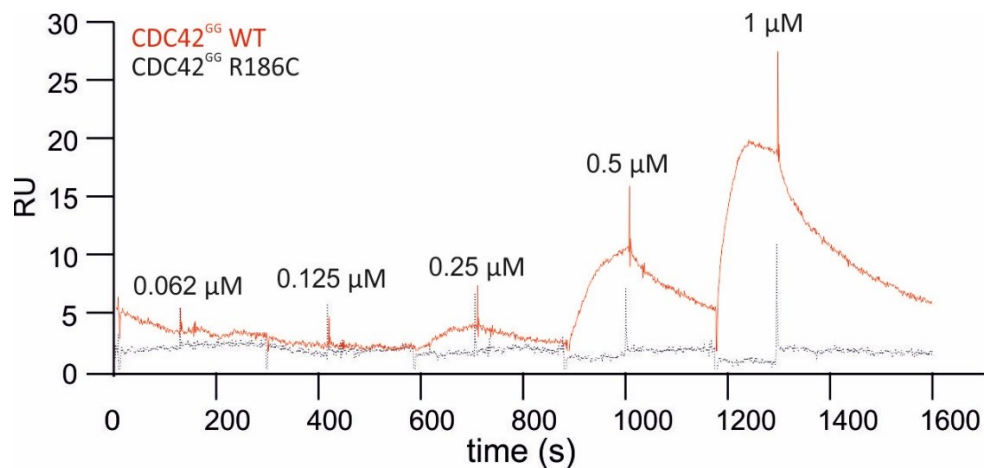


Figure 22 A representative surface plasmon resonance (SPR) analysis of GDI interaction with CDC42 wild type versus CDC42^{R186C}. The data showed that CDC42^{GG} wild type binding to the immobilized GST-GDI shows a K_d of 55 μM (global fitting). On the other hand, titration of CDC42^{R186C} showed no binding response. In good agreement with liposome binding experiment showed in Fig.1D, CDC42^{GG} R186C has lower binding affinity toward GDI in comparison with CDC42 wild type.

3.2.2. New chemical compound inhibits GDI interaction with RHO GTPase

Hedgehog pathway is a master regulator of developmental processes. In adult, hedgehog pathway controls tissue homeostasis and repair mechanisms. Dysregulation of this pathway in human leads to uncontrolled growth and cancer. Therefore, there is an urgent need for a drug to target this pathway. Non-canonical hedgehog signaling get activated through G-protein-coupled receptor, which activates monomeric G proteins like RHOA and RAC1. Here, a chemical compound (Rhonin) was found as a hedgehog inhibitor (data are not shown). Further biochemical analysis indicated that Rhonin interacts with RHOGDI1 and through this protein impacts RHO signaling.

Florescent anisotropy measurement indicated that Rhonin interferes with the GDI1 interaction and function. 1 μM bodipy-coupled Rhonin was added to a cuvette and increasing concentrations of GDI was titrated till signal get saturated. Finally, anisotropy versus concentration was curved and fitted to a non-linear model in order to measure K_d of the direct interaction between Rhonin and

GDI (Fig. 23). Rhonin binds to RAC1 with a K_d of 7.2 μM . To analyze the binding interface of the chemical compound to GDI, Rhonin was incubated with GDI till signal is equilibrated. Next, addition of RAC1^{GG} led to sharp decrease of signal, which was due to Rhonin displacement in the presence of RAC1^{GG}. Using non-prenylated RAC1 indicates that geranylgeranyl moiety is crucial for Rhonin displacement (Fig. 24).

To analyze the impact of Rhonin on function, the displacement of RHO proteins from synthetic liposome by GDI was measured. Western blotting (WB) using anti-RAC1 and anti-GST antibodies, showed that RAC1 (1 μM) efficiently bound to liposomes and was sedimented to the pellet fraction. Incubation of liposome-bound RAC1 with GST-GDI led to displacement of RAC1 (Fig. 25a). Next, GDI function was measured after incubation with Rhonin. Obtained data indicates that Rhonin blocks GDI function. To avoid aggregate formation during the incubation of the chemical compound with proteins, floatation assay was performed. In this method, proteins are separated based on their density during a gradient centrifugation step. Liposome bound proteins have a lower density compared to liposome-free proteins and float to the upper phase. liposome-associated RAC1 was detected in the upper liposome-containing phase using 5% fluorescent NDB-PE but not if the experiments were performed in the presence of GST-GDI1. This function was blocked in the presence of 50 μM Rhonin, strongly supporting the notion that Rhonin binds GDI1 and interferes with its association with geranylgeranylated RAC1 (Fig. 25b). Using liposome sedimentation assay, membrane cycling of RHOA and CDC42 by GDI was also analyzed in the presence of Rhonin and it showed that Rhonin could interfere with all three RHO GTPases in cell free condition (Fig. 25c, d).

To monitor the kinetics of Rhonin inhibition SPR method was used. Synthetic PI(4, 5)P₂-rich liposomes were immobilized on the L1 sensor chip (Fig. 26). An increase in response units (RU) remained stable after washing with HEPES buffer (20 mM HEPES, 150 mM NaCl, 5 mM MgCl₂, 3 mM DTT), containing 10 nM NaOH. Next, geranylgeranylated, GDP-bound RAC1 (RAC1^{GG}-GDP) was loaded on the liposome-immobilized L1 sensor chip, which resulted in a massive RU increase upon RAC1 binding to the liposomes

monitored. The signal remained relatively stable after washing with buffer but rapidly decreased upon injection of 25 μM GDI1. Addition of GDI1 displaced liposome-bound RAC1 significantly slower when GDI1 was mixed with 50 μM Rhonin as compared to a mixture of GDI1 and an inactive Rhonin derivative 1025 (50 μM). Calculated rate constants by mono-exponential fitting of

RU decays were 0.002 and 0.0032 s^{-1} for GDI-mediated RAC1 displacement from the liposomes in the presence of Rhonin and 1025, respectively (Fig. 27).

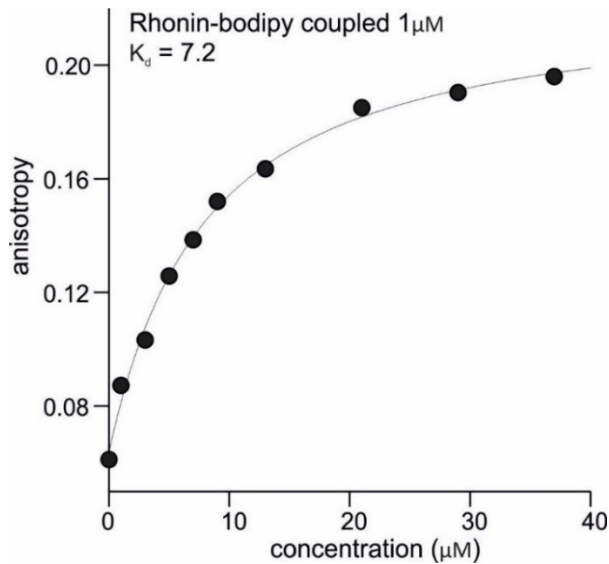


Figure 23 Affinity of interaction of bodipy-coupled Rhonin versus different GDI concentrations indicated an affinity of $7.2 \mu\text{M}$.

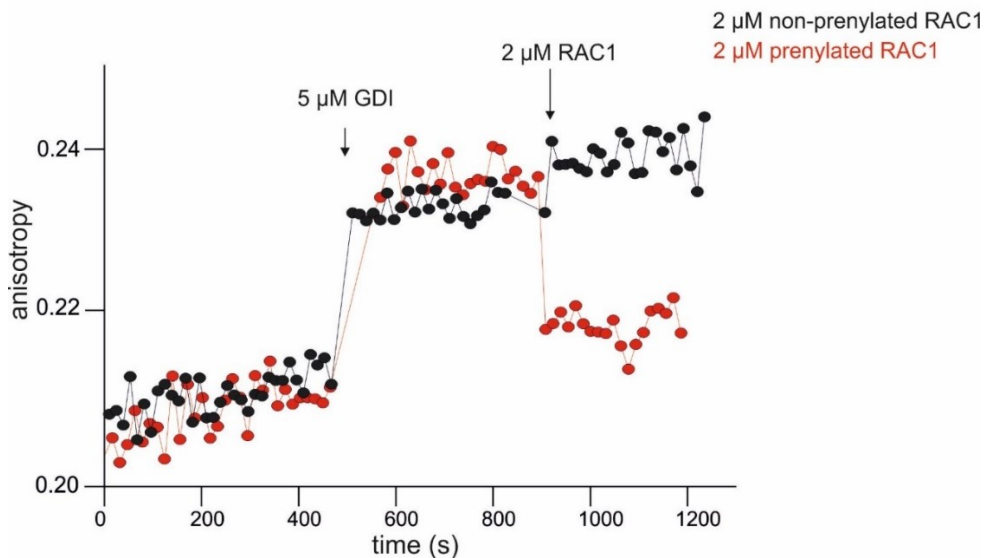


Figure 24 Prenylated RAC1 interferes with Rhonin binding to GDI. $2 \mu\text{M}$ bodipy-coupled Rhonin was diluted in buffer (20 mM HEPES, 150 mM NaCl, 3 mM DTT, 5 mM MgCl_2) at pH 7.4. Anisotropy was monitored till signal got stable, then $5 \mu\text{M}$ GDI was added to the cuvette. When it reaches equilibrium, $2 \mu\text{M}$ of prenylated (red dot) or non-prenylated (black dot) RAC1 was added to the cuvette. Data showed that Rhonin did not interfere with binding interface of non-prenylated RAC1 but prenylated one. In fact, this shows that Rhonin binds to the hydrophobic pocket of GDI where it could interfere with geranylgeranyl moiety.

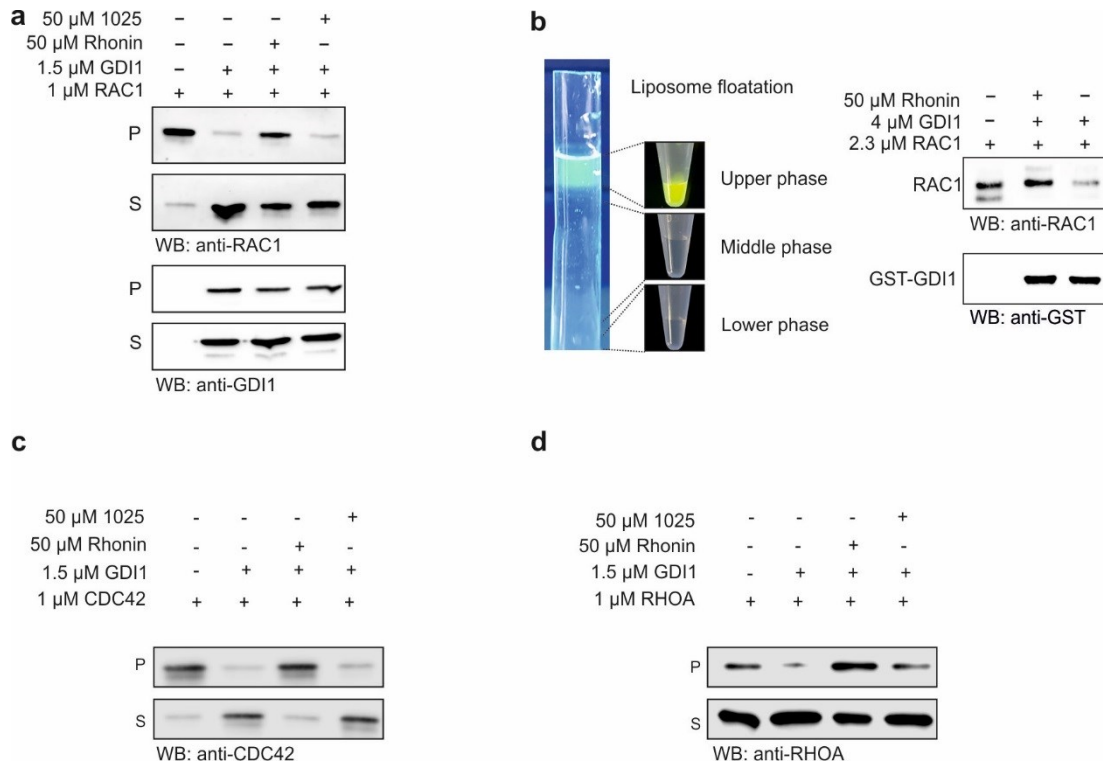


Figure 25 Analysis of inhibitory effect of Rhonin on GDI function over RHO GTPases. **a**, RAC1 displacement from the liposomes by GST-RHO GDI1 in the presence and absence of Rhonin was analyzed by liposome floatation assay. **b**, in floatation assay, liposome-associated RAC1 was detected in the upper liposome-containing phase using fluorescent NDB-PE but not if the experiments were performed in the presence of GST-RHO GDI1. **c** and **d**, using liposome sedimentation assay, membrane cycling of RHOA and CDC42 by GDI was also analyzed in the presence of Rhonin and it showed that Rhonin could interfere with all three RHO GTPases under cell free condition.

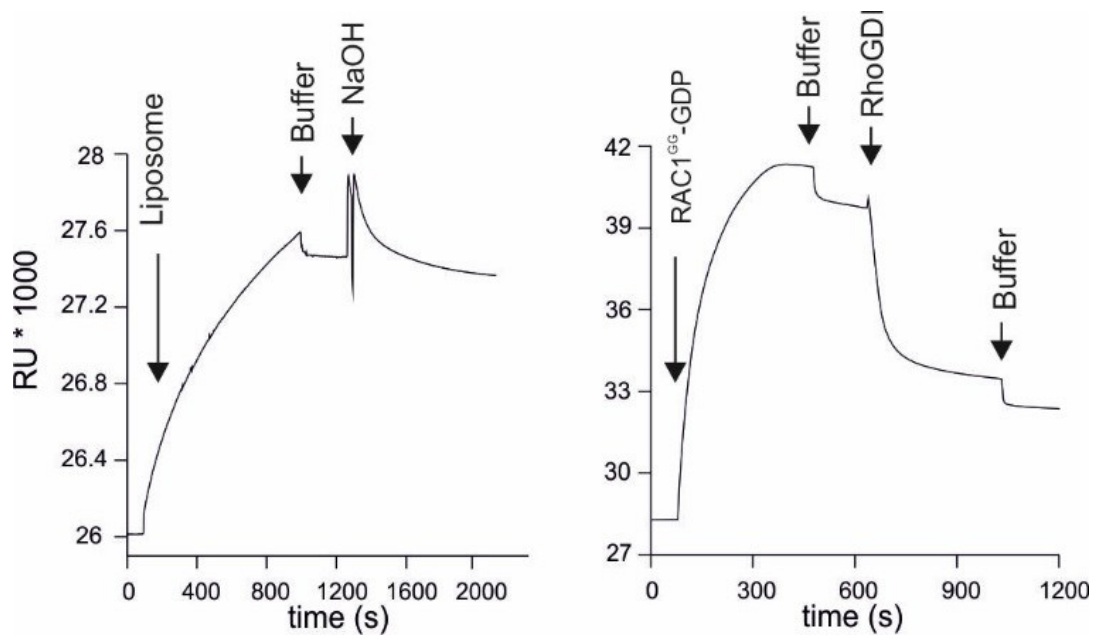


Figure 26 Surface plasmon resonance (SPR) measurement. Synthetic liposomes (contain 20% PS, 5% cholesterol, 5% PI(4, 5)P₂, 20% PE, and 50% PC) were immobilized on L1 chip (left panel). Kinetic parameter of interaction between immobilized GST-GDI and RAC1^{GG} is shown in right panel.

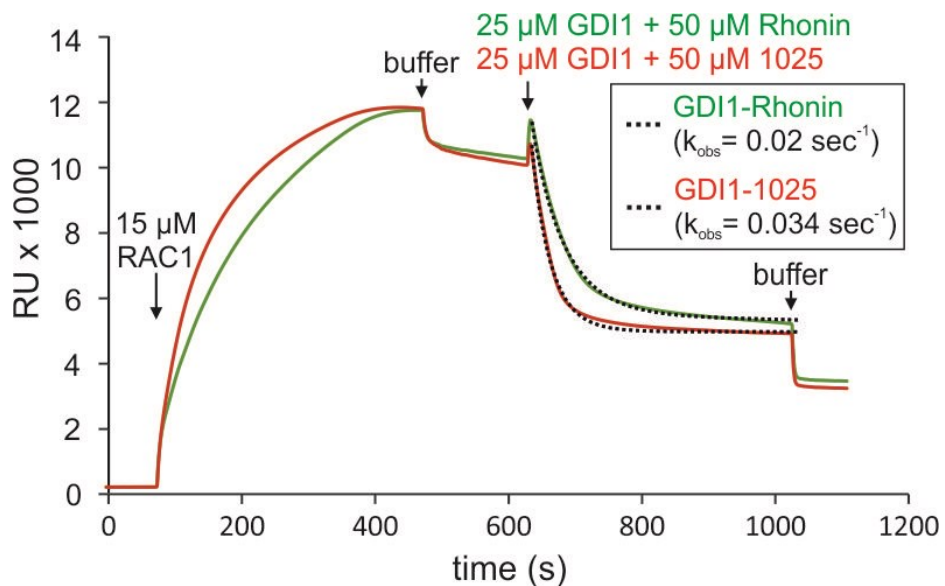


Figure 27 SPR analysis of Rhonin and its inactive variant 1025 on kinetic of GDI interaction with RAC1^{GG}. RAC1^{GG} injected to immobilized liposomes surface and GDI (preincubated with Rhonin or 1025) was added to measure the kinetics of RAC1^{GG} displacement by GDI.

4. Discussion

The large number of regulators including 66 GAPs, 74 GEFs and 3 GDIs provide a tight spatio-temporal control of RHO signaling. Therefore, functional diversities of RHO signaling is highly regulated by its subcellular localization and its activation status. On the one hand, the large number of GAPs and GEFs, containing various individual domains, specifically localized at different compartments in cell. On the other hand, GEFs have a high specificity towards different RHO proteins (Jaiswal et al., 2011). Accordingly, specificity of GEFs could explain the selective activation of RHO signaling. GEFs are generally in an autoinhibition state. Activation of various cellular receptors could release the autoinhibition state of GEFs and bring them in a close vicinity of RHO proteins. Consequently, Activated GEFs interact and turn-on specific RHO proteins which leads to a downstream signaling cascade of (Buchsbaum, 2007). Timing of the cycle in on-state is then regulated by the GAP family of proteins. They inactivate RHO proteins by hydrolyzing GTP to GDP. To avoid the reactivation of RHO proteins, GDI binding results in translocation to the cytosol. In the absence of GDI, cytosolic RHO^{GG} proteins are not stable and get targeted for proteasomal degradation (Boulter et al., 2010). To reactivate RHO proteins, it should be first released from GDI to be available for GEF in the proper position into a cell. Therefore, unspecific release of RHO from GDI complex could not explain the specific activation various RHO signaling. Herein, we focused on investigation of GDI mechanism of function over various RHO proteins. Furthermore, phosphorylation of GDI could provide a specific interaction between GDI and GTPases. For instance, phosphorylation of GDI at position Ser101 and Ser174 reduced the affinity of RAC1 toward GDI but not RHOA (DerMardirossian et al., 2004). Moreover, phosphorylation of Ser188 in RHOA increases its binding to GDI (Rolli-Derkinderen et al., 2005). Although, there are other mechanisms explained through direct interaction of releasing factors to GDI and other types of posttranslational modifications, the mechanism of GDI binding toward RHO proteins is still not clear. To gain insight into the function of GDI1, we analyzed GDI binding and the presence of RHO membrane displacement.

GDI1 displaces RHO GTPases from membrane *in vitro* and *in vivo* (Moissoglu et al., 2006; Pick et al., 1993; Ugolev et al., 2008). Furthermore, previous work has shown that GDI is able to dislodge prenylated RAC1 from PIP₂ containing liposome (Ugolev et al., 2008; Zhang et al., 2014). In this work, we were able to reconstitute efficiently the activity of GDI as displacement factor (Figs. 8 and 9). Prenylated RHO proteins, proofed with mass spectrometry analysis (Fig. 5), interacts and localizes on PI(4, 5)P₂ rich liposome (Radius of 100 nm). Addition of GDI, displaces

RHO^{GG} from liposomes into a soluble fraction (Fig. 8). In addition, the kinetics of this cycle of liposome and soluble exchange, was measured with different methods including SPR and stopped flow instruments. Using mant-dGDP labeled RAC1 reveals that the binding of RHO to GDI is tightly dependent on the HVR of the RHO proteins (Fig. 11). Based on obtained data, non-prenylated RAC1 interact with a nanomolar affinity (300 nM) to GDI whereas a C-terminal truncated construct of RAC1 was not able to interact. To understand the interface region between GDIs and RHO proteins, we analyzed the protein-protein interaction matrix based on available crystal structures of GDI/RHO GTPase (Fig. 2). This analysis revealed a conserved interface between GDIs and GTPases (Ueyama et al., 2013). Central residues of GDI including D45, D185, and the residues of RHO like Y64, R66 are identical between all members of the family, whereas, k_{obs} measurement shows magnificent differences between the interaction of the individual full length RHO GTPases and GDI (Fig. 11). In other words, the heterogeneous pattern of k_{obs} proposed a selective interaction (in term of affinity and kinetics) with GDI (Fig. 28). Nanomolar affinity of non-prenylated RHO proteins suggests a new role for GDI as a regulator of prenylation (Tnimo et al., 2014). Moreover, there are other proteins, which bind to the polybasic region of RHO proteins and regulate their localization and activation mode. For instance, there are two splice variants of smgGDS 558 and 607 which interact with prenylated and non-prenylated form of RHO proteins, respectively (Lanning et al., 2004). smgGDS 607 variant enhances the prenylation of RHO proteins through interaction with the polybasic region of non prenylated RHO proteins (Lanning et al., 2004). In this way, smgGDS regulates localization and trafficking of RHO proteins (Lanning et al., 2004). Polybasic region also contains a nuclear localization signal (NLS) which leads to nuclear positioning of RAC1 whereas overexpressed RHOA localized in cytosol (Wu et al., 2008). In general, polybasic region plays a crucial role in regulation of RHO localization through specific ranges of binding partners. Understanding the mechanism of interaction of GDI with prenylated and non-prenylated RHO proteins, provide a deeper view of RHO trafficking that leads our attention toward the role of HVR as trafficking code. Taken together, these analyzes suggest a selective behavior for GDI that highlights the role of HVR and its binding partner as critical factor in RHO protein localization.

The HVR sequence contains polybasic residues, which have a diverse pattern between various family members. Crystal structure and RAC1 and GDI indicates that mentioned positively charged residues are positioned in close vicinity to GDI, where it is enriched by negatively charged residues of GDI including E163 and E164 (Fig. 12a). Furthermore, RAC1 contains a sequence of six positive R/K residues to guarantee the interaction with GDI. Mutating these residues into

negatively charged amino acids leads to repulsion of the proteins and impaired interaction (Fig. 13b). HVR is also involved in membrane binding due to its electrostatic nature. Polybasic region of HVR contains positively charged residues, which could be positioned in the close proximity of negatively charged membrane lipids like phosphatidylserine and phosphatidylinositol phosphate derivatives (Jang et al., 2015). In fact, to properly localize on the membrane, lipid modification alone is not efficient and other interfaces e.g. the polybasic region contribute to a lower dissociation rate (Resh, 2006).

Synthesis of biomimetic liposomes, using various lipids with defined concentration followed by homogenizing them into a defined size by extruders, provides a proper membrane to analyze membrane interaction of proteins. Phosphatidylserine (PS) and phosphatidylinositol 4,5-bisphosphate (PIP₂) are positioned in the inner leaflet of the cellular plasma membrane, regarding some exceptions like platelet activation, and give a negative-charged nature to the cytosolic surface of plasma membrane (van den Bogaart et al., 2011). On the other hand, phosphatidylethanolamine generates curvature in the membranes due to its small head group, which allows its positioning in the inner leaflet of membrane in order to facilitate curvature formation (McMahon and Boucrot, 2015). This type of synthetic liposomes is proper to analyze electrostatics, hydrophobic and curve-dependent binding forces. Kinetic analysis of different RHO constructs indicates that the membrane binding of RAC1 is nucleotide dependent. RAC1^{GDP} binds with a three-fold higher affinity to GDI ($K_d = 0.34 \mu\text{M}$) compared to RAC1^{GppNHp} ($K_d = 1 \mu\text{M}$) (Table 3). Moreover, prenylated RAC1 with a K_d of 33 nM has a ten-fold higher affinity than the non-prenylated one. This difference is mainly due to a ten-fold decrease in k_{off} of RAC1^{GG} compared to RAC1 (Table 3). Further addition of GDI, increases k_{off} of RAC1^{GG} up to fifty-fold (Fig. 15). Based on the fact that geranylgeranyl moiety gives a membrane-association potential to RHO proteins, there is a call for GDI as a membrane displacement factor to increase RHO dynamic between membrane and cytosol (Dovas and Couchman, 2005). Comparing RAC1 with RAC2 (Table 3) revealed the impact of polybasic region as a second membrane associating factor which does not only play a role in membrane association but also regulates RHO interaction with membrane trafficking factors like smgGDS and GDI (Jang et al., 2015; Lanning et al., 2004). In detail, beside geranylgeranyl moiety there is a second membrane binding signal upstream of CAAX sequence such as polybasic and palmitoylation site (Michaelson et al., 2001). Contribution of both polybasic and geranylgeranyl moiety regulates the kinetic of RHO membrane cycling.

Interaction and function of GDI towards newly discovered CDC42 (R186C) mutant supports our model in which mutation of positive charged residues in HVR of CDC42 is not efficiently binds to

GDI compared to its wild type construct (Fig. 21). This *de novo* CDC42 mutant (R186C) is responsible for an autoinflammatory disorder, resulting in mislocalization of CDC42 and accumulation at the Golgi (data not shown). Based on CDC42/GDI crystal structure (Bucki et al., 2001; Hoffman et al., 2000), R186 is in close vicinity to the negatively charged residues in GDI. Its mutation to Cysteine reduces the electrostatic potential of CDC42 for GDI binding. Following our model, this electrostatic interaction between polybasic region of RHO proteins and GDI provides a strong interface, which makes GDI a selective displacement regulator. Sedimentation of CDC42 wild type and mutant indicates that mutation in R186 interferes with CDC42 binding ability to GDI (Fig. 21b). Further kinetic analysis of CDC42 wild type and R186C with SPR showed the GDI insensitivity of the mutant (Fig. 22). In this experiment, affinity of the measurement is not comparable with previously data due to the different set up that was used. CDC42 mutant did not bind to the GDI up to 1 μ M concentration of higher concentration of CDC42^{R186C} led to bulk effect (Fig. 22). Then, we could not use higher concentration of CDC42 due to its bulky effect here (Fig. 22). The proposed model showed that mutation in polybasic region of RHO proteins could dysregulate localization of function of RHO signaling.

GDI is a negative regulator of RHO GTPases and its specific inhibition was suggested as a target in cancer therapy (Harding and Theodorescu, 2010). Hedgehog is one of the cancer related pathways and aberrant regulation of hedgehog pathway in adult leads to cancer (Gupta et al., 2010). Recently, a new chemical compound called Rhonin was identified targeting hedgehog pathway (data are not shown). Further analysis showed that Rhonin binds GDI and upregulates RHO proteins (Fig. 23). Furthermore, it has been shown that RHO proteins are downstream of hedgehog in a non-canonical pathway (Ho Wei et al., 2018). Direct binding measurement indicates an affinity of 7.2 μ M for GDI, which is not a strong binding affinity in physiological condition. Addition of non-prenylated RAC1 leads to formation of a tertiary complex between RAC1/GDI/Rhonin while addition of prenylated RAC1 leads to the displacement of Rhonin from GDI, which strongly suggests that Rhonin is positioned in hydrophobic cavity to GDI, where the interface of geranylgeranyl moiety is located. Liposome sedimentation assay of GDI, performed in the absence and presence of Rhonin indicates the inhibitory effect of this chemical compound on the GDI function (Fig. 25). Generally, mechanistic analysis suggests an inhibition of the hydrophobic pocket of GDI which interferes within RAC1^{GG} binding (Fig. 24) and due to its low affinity it is displaced in the presence of RAC1^{GG} which has high nanomolar affinity for GDI (63 nM, Table 3) suggests existence of other interfaces between GDI and RHO (Figs. 24 and 28). It means, other interfaces between RAC1 and GDI makes it difficult to target with a compound which

targets hydrophobic interface of RAC1 geranylgeranyl and GDI hydrophobic pocket. As indicated for CDC42^{R186C}, the polybasic region is more crucial regarding GDI binding than the geranylgeranyl interaction with the hydrophobic pocket of GDI. Generally, a point mutation in HVR can profoundly disrupt GDI-dependent cycling of RHO (Fig. 22) compared to the Rhonin, which targets and disrupts the hydrophobic binding interface (Fig. 24).

In summary, the hydrophobic C-terminal domain of GDI forms a immunoglobulin-like domain which completely cover the lipid moiety of RHO proteins (Grizot et al., 2001). Previous studies suggest that GG moiety interaction with the hydrophobic pocket of GDI is crucial for its displacement (Dransart et al., 2005). The missing part in this proposed model is the transition state leading to complete displacement of GTPase from membrane (Fig. 28). We have shown that, upon the inhibition of the hydrophobic pocket in GDI by GGpp analogue, GDI is still able to function efficiently (Fig. 9). Moreover, N-terminal region of GDI forms a short helix (10-15 aa) upon binding to the GTPases which could interfere as well with membrane binding surface of HVR region (Golovanov et al., 2001; Keep et al., 1997; Scheffzek et al., 2000). Based on our results, not only N-terminal regions of GDI but also negatively charged region corresponding to the EE163-164 are involved in displacement of GTPase from the membrane (Fig. 14). Upon interaction of GDI with the switch region of GTPase, N-terminal part of GDI extends the binding interface by interfering with electrostatic interactions between HVR and negative surface of the membrane and promotes the extraction of geranylgeranyl moiety from membrane (Fig. 14). Kinetic data shows that RHO interaction with membrane is tightly regulated by geranylgeranyl moiety and HVR. Taken together, GDI interaction with different constructs of RAC1 indicates that in addition of the geranylgeranyl moiety, HVR is a central interface between GDI and RHO complex, which could lead to a selective kinetics of interaction. In addition, HVR is also able to translocate to the negatively charged membrane and increase the association rate constant of RAC1 compared to RAC2 (Table 4). These findings are in agreement with liposomal pull down experiment which shows displacement of GTPases with less positive charges in the HRV (CDC42) is more efficient compare to those with more positive charges in the HVR (like RAC1 and RHOA) (fig 17). Our proposed mechanism of selective RHO membrane displacement and localization paved the road toward understanding the spatio-temporal regulation of RHO signaling.

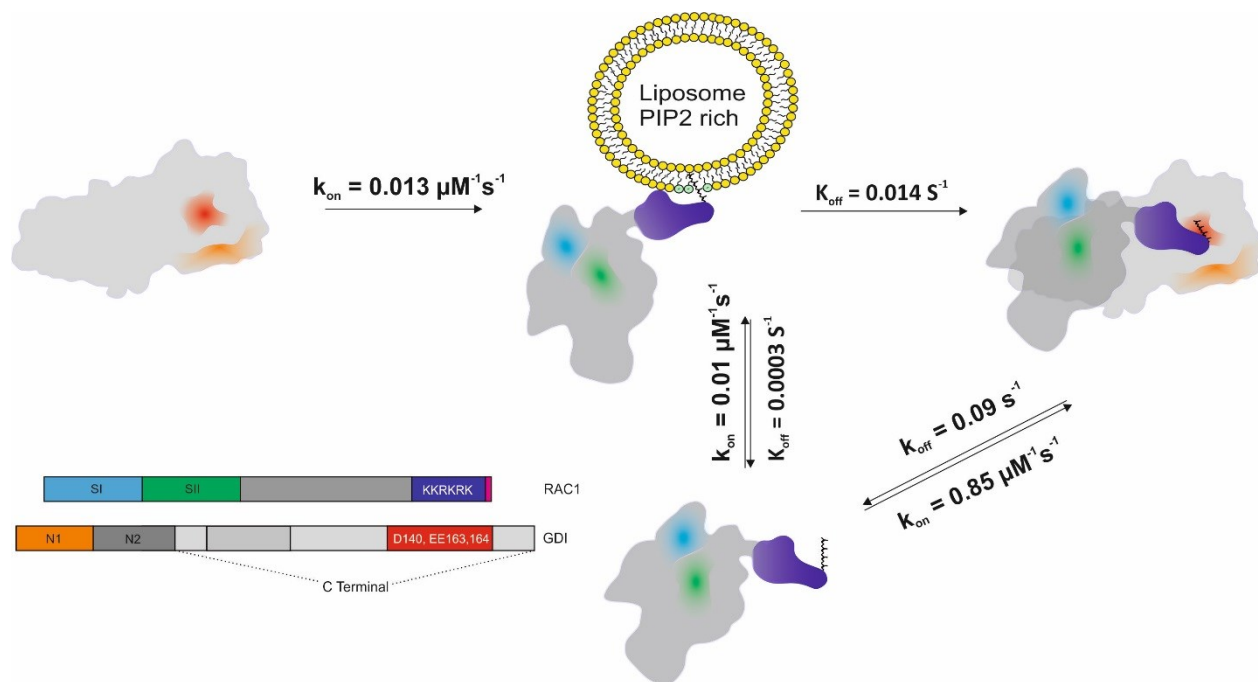


Figure 28 Proposed mechanism of GDI function as a membrane displacement factor. Kinetic parameters of RAC1 cycling on the liposome are obtained from SPR data, which are represented in tables 3 and 4. Moreover, GDI/RAC1 cycling in solution (without membrane) obtained from stopped flow measurements because both proteins have three-dimensional movement. RAC1 dissociates with a k_{off} 0.0003 s^{-1} but addition of GDI increase this rate constant to 0.014 s^{-1} .

Acknowledgements

I would like to thank my supervisor, Prof. Reza Ahmadian, for the patient guidance, encouragement and advice he has provided throughout my time, especially during the first year of my PhD, as his student. I would also like to thank the members and staff at Heinrich-Heine-University who helped me specially Prof. Jürgen Scheller, Dr. Roland Piekorz and Dr. Radovan Dvorsky. In particular, I would like to thank my friends Oliver Krumbach, Marcel Buchholzer, Jana Lissy, Neda Jasemi, Ali Salehzadeh Yazdi, Kazem Nouri, Nastaran Fazel, Erika Engelowski, Jens Moll and Ehsan Amin for suggestions they made regarding my thesis and presentations and specially those moments that we share on a table to drink. Other group members and the support of Ilse Mayer, Feri and Petra Oprea Jeremic are highly acknowledged. I thank also Dr. Si-Cai Zhang for his efforts in establishing various materials and methods, which were used, in my thesis.

5. References

- Aicart-Ramos, C., R.A. Valero, and I. Rodriguez-Crespo. 2011. Protein palmitoylation and subcellular trafficking. *Biochimica et Biophysica Acta (BBA) - Biomembranes*. 1808:2981-2994.
- Allal, C., A. Pradines, A.D. Hamilton, S.M. Sebti, and G. Favre. 2002. Farnesylated RhoB prevents cell cycle arrest and actin cytoskeleton disruption caused by the geranylgeranyltransferase I inhibitor GGTI-298. *Cell Cycle*. 1:430-437.
- Amin, E., M. Jaiswal, U. Derewenda, K. Reis, K. Nouri, K.T. Koessmeier, P. Aspenstrom, A.V. Somlyo, R. Dvorsky, and M.R. Ahmadian. 2016. Deciphering the Molecular and Functional Basis of RHOGAP Family Proteins: A SYSTEMATIC APPROACH TOWARD SELECTIVE INACTIVATION OF RHO FAMILY PROTEINS. *J Biol Chem*. 291:20353-20371.
- Ashar, H.R., L. James, K. Gray, D. Carr, M. McGuirk, E. Maxwell, S. Black, L. Armstrong, R.J. Doll, A.G. Taveras, W.R. Bishop, and P. Kirschmeier. 2001. The farnesyl transferase inhibitor SCH 66336 induces a G(2) --> M or G(1) pause in sensitive human tumor cell lines. *Exp Cell Res*. 262:17-27.
- Baron, R., E. Fourcade, I. Lajoie-Mazenc, C. Allal, B. Couderc, R. Barbaras, G. Favre, J.C. Faye, and A. Pradines. 2000. RhoB prenylation is driven by the three carboxyl-terminal amino acids of the protein: evidenced in vivo by an anti-farnesyl cysteine antibody. *Proc Natl Acad Sci U S A*. 97:11626-11631.
- Baschieri, F., S. Confalonieri, G. Bertalot, P.P.D. Fiore, W. Dietmaier, M. Leist, P. Crespo, I.G. Macara, and H. Farhan. 2014. Spatial control of Cdc42 signalling by a GM130–RasGRF complex regulates polarity and tumorigenesis. *Nature Communications*. 5:ncomms5839.
- Bigay, J., J.F. Casella, G. Drin, B. Mesmin, and B. Antonny. 2005. ArfGAP1 responds to membrane curvature through the folding of a lipid packing sensor motif. *EMBO J*. 24:2244-2253.
- Bos, J.L., H. Rehmann, and A. Wittinghofer. 2007. GEFs and GAPs: critical elements in the control of small G proteins. *Cell*. 129:865-877.
- Boulter, E., R. Garcia-Mata, C. Guilluy, A. Dubash, G. Rossi, P.J. Brennwald, and K. Burridge. 2010. Regulation of Rho GTPase crosstalk, degradation and activity by RhoGDI1. *Nat Cell Biol*. 12:477-483.
- Brunet, N., A. Morin, and B. Olofsson. 2002. RhoGDI-3 Regulates RhoG and Targets This Protein to the Golgi Complex Through its Unique N-Terminal Domain. *Traffic*. 3:342-358.
- Buchsbaum, R.J. 2007. Rho activation at a glance. *J Cell Sci*. 120:1149-1152.
- Bucki, R., P.A. Janmey, R. Vegners, F. Giraud, and J.-C. Sulpice. 2001. Involvement of Phosphatidylinositol 4,5-Bisphosphate in Phosphatidylserine Exposure in Platelets: Use of a Permeant Phosphoinositide-Binding Peptide†. *Biochemistry*. 40:15752-15761.
- de Leon-Bautista, M.P., M.D. Cardenas-Aguayo, D. Casique-Aguirre, M. Almaraz-Salinas, S. Parraguirre-Martinez, A. Olivo-Diaz, M.D. Thompson-Bonilla, and M. Vargas. 2016. Immunological and Functional Characterization of RhoGDI3 and Its Molecular Targets RhoG and RhoB in Human Pancreatic Cancerous and Normal Cells. *PLoS One*. 11:e0166370.
- DerMardirossian, C., and G.M. Bokoch. 2005. GDIs: central regulatory molecules in Rho GTPase activation. *Trends Cell Biol*. 15:356-363.
- DerMardirossian, C., G. Rocklin, J.Y. Seo, and G.M. Bokoch. 2006. Phosphorylation of RhoGDI by Src regulates Rho GTPase binding and cytosol-membrane cycling. *Mol Biol Cell*. 17:4760-4768.
- DerMardirossian, C., A. Schnelzer, and G.M. Bokoch. 2004. Phosphorylation of RhoGDI by Pak1 mediates dissociation of Rac GTPase. *Mol Cell*. 15:117-127.

- Dovas, A., and J.R. Couchman. 2005. RhoGDI: multiple functions in the regulation of Rho family GTPase activities. *Biochem J.* 390:1-9.
- Dransart, E., B. Olofsson, and J. Cherfils. 2005. RhoGDIs revisited: novel roles in Rho regulation. *Traffic.* 6:957-966.
- Dvorsky, R., and M.R. Ahmadian. 2004. Always look on the bright side of Rho: structural implications for a conserved intermolecular interface. *Embo Rep.* 5:1130-1136.
- Ellerbroek, S.M., K. Wennerberg, and K. Burridge. 2003. Serine phosphorylation negatively regulates RhoA in vivo. *J Biol Chem.* 278:19023-19031.
- Fidyk, N.J., and R.A. Cerione. 2002. Understanding the Catalytic Mechanism of GTPase-Activating Proteins: Demonstration of the Importance of Switch Domain Stabilization in the Stimulation of GTP Hydrolysis†. *Biochemistry.* 41:15644-15653.
- Forget, M.-A., R.R. Desrosiers, D. Gingras, and R. BÉLiveau. 2002. Phosphorylation states of Cdc42 and RhoA regulate their interactions with Rho GDP dissociation inhibitor and their extraction from biological membranes. *Biochemical Journal.* 361:243-254.
- Gao, J., J. Liao, and G.Y. Yang. 2009. CAAX-box protein, prenylation process and carcinogenesis. *Am J Transl Res.* 1:312-325.
- Garcia-Mata, R., E. Boulter, and K. Burridge. 2011. The 'invisible hand': regulation of RHO GTPases by RHOGDIs. *Nat Rev Mol Cell Biol.* 12:493-504.
- Ghosh, P. 2015. Heterotrimeric G proteins as emerging targets for network based therapy in cancer: End of a long futile campaign striking heads of a Hydra. *Aging (Albany NY).* 7:469-474.
- Gibson, R.M., P.N. Gandhi, X. Tong, J. Miyoshi, Y. Takai, M. Konieczkowski, J.R. Sedor, and A.L. Wilson-Delfosse. 2004. An activating mutant of Cdc42 that fails to interact with Rho GDP-dissociation inhibitor localizes to the plasma membrane and mediates actin reorganization. *Experimental Cell Research.* 301:211-222.
- Gibson, R.M., and A.L. Wilson-Delfosse. 2001. RhoGDI-binding-defective mutant of Cdc42Hs targets to membranes and activates filopodia formation but does not cycle with the cytosol of mammalian cells. *Biochemical Journal.* 359:285-294.
- Golovanov, A.P., T.H. Chuang, C. DerMardirossian, I. Barsukov, D. Hawkins, R. Badii, G.M. Bokoch, L.Y. Lian, and G.C. Roberts. 2001. Structure-activity relationships in flexible protein domains: regulation of rho GTPases by RhoGDI and D4 GDI. *J Mol Biol.* 305:121-135.
- Griner, E.M., M.E. Churchill, D.L. Brautigan, and D. Theodorescu. 2013. PKC α phosphorylation of RhoGDI2 at Ser31 disrupts interactions with Rac1 and decreases GDI activity. *Oncogene.* 32:1010-1017.
- Griner, E.M., and D. Theodorescu. 2012. The faces and friends of RhoGDI2. *Cancer Metastasis Rev.* 31:519-528.
- Grizot, S., J. Fauré, F. Fieschi, P.V. Vignais, M.C. Dagher, and E. Pebay-Peyroula. 2001. Crystal Structure of the Rac1-RhoGDI Complex Involved in NADPH Oxidase Activation†,‡. *Biochemistry.* 40:10007-10013.
- Gupta, S., N. Takebe, and P. Lorusso. 2010. Targeting the Hedgehog pathway in cancer. *Ther Adv Med Oncol.* 2:237-250.
- Gureasko, J., W.J. Galush, S. Boykevich, H. Sondermann, D. Bar-Sagi, J.T. Groves, and J. Kuriyan. 2008. Membrane-dependent signal integration by the Ras activator Son of sevenless. *Nat Struct Mol Biol.* 15:452-461.
- Hall, A. 2005. Rho GTPases and the control of cell behaviour. *Biochem Soc Trans.* 33:891-895.
- Hall, A. 2012. Rho family GTPases. *Biochem Soc Trans.* 40:1378-1382.
- Harding, M.A., and D. Theodorescu. 2010. RhoGDI signaling provides targets for cancer therapy. *Eur J Cancer.* 46:1252-1259.

- Hemsath, L., R. Dvorsky, D. Fiegen, M.F. Carlier, and M.R. Ahmadian. 2005. An electrostatic steering mechanism of Cdc42 recognition by Wiskott-Aldrich syndrome proteins. *Mol Cell*. 20:313-324.
- Ho Wei, L., M. Arastoo, I. Georgiou, D.R. Manning, and N.A. Riobo-Del Galdo. 2018. Activation of the Gi protein-RHOA axis by non-canonical Hedgehog signaling is independent of primary cilia. *PLoS One*. 13:e0203170.
- Hodge, R.G., and A.J. Ridley. 2016. Regulating Rho GTPases and their regulators. *Nat Rev Mol Cell Biol*. 17:496-510.
- Hoffman, G.R., N. Nassar, and R.A. Cerione. 2000. Structure of the Rho Family GTP-Binding Protein Cdc42 in Complex with the Multifunctional Regulator RhoGDI. *Cell*. 100:345-356.
- Ignatev, A., S. Kravchenko, A. Rak, R.S. Goody, and O. Pylypenko. 2008. A structural model of the GDP dissociation inhibitor rab membrane extraction mechanism. *J Biol Chem*. 283:18377-18384.
- Jaiswal, M., R. Dvorsky, and M.R. Ahmadian. 2013a. Deciphering the molecular and functional basis of Dbl family proteins: a novel systematic approach toward classification of selective activation of the Rho family proteins. *J Biol Chem*. 288:4486-4500.
- Jaiswal, M., R. Dvorsky, E. Amin, S.L. Risse, E.K. Fansa, S.C. Zhang, M.S. Taha, A.R. Gauhar, S. Nakhaei-Rad, C. Kordes, K.T. Koessmeier, I.C. Cirstea, M.A. Olayioye, D. Haeussinger, and M.R. Ahmadian. 2014. Functional crosstalk between Ras and Rho pathways: p120RasGAP competitively inhibits the RhoGAP activity of Deleted in Liver Cancer (DLC) tumor suppressors by masking its catalytic arginine finger. *J Biol Chem*. 24:Epub ahead of print.
- Jaiswal, M., E.K. Fansa, R. Dvorsky, and M.R. Ahmadian. 2013b. New insight into the molecular switch mechanism of human Rho family proteins: shifting a paradigm. *Biol. Chem*. 394:89-95.
- Jaiswal, M., L. Gremer, R. Dvorsky, L.C. Haeusler, I.C. Cirstea, K. Uhlenbrock, and M.R. Ahmadian. 2011. Mechanistic insights into specificity, activity, and regulatory elements of the regulator of G-protein signaling (RGS)-containing Rho-specific guanine nucleotide exchange factors (GEFs) p115, PDZ-RhoGEF (PRG), and leukemia-associated RhoGEF (LARG). *J Biol Chem*. 286:18202-18212.
- Jang, H., S.J. Abraham, T.S. Chavan, B. Hitchinson, L. Khavrutskii, N.I. Tarasova, R. Nussinov, and V. Gaponenko. 2015. Mechanisms of membrane binding of small GTPase K-Ras4B farnesylated hypervariable region. *J Biol Chem*. 290:9465-9477.
- Karnovsky, M.J., A.M. Kleinfeld, R.L. Hoover, and R.D. Klausner. 1982. The concept of lipid domains in membranes. *J Cell Biol*. 94:1-6.
- Keep, N.H., M. Barnes, I. Barsukov, R. Badii, L.-Y. Lian, A.W. Segal, P.C.E. Moody, and G.C.K. Roberts. 1997. A modulator of rho family G proteins, rhoGDI, binds these G proteins via an immunoglobulin-like domain and a flexible N-terminal arm. *Structure*. 5:623-633.
- Kuhlmann, N., S. Wroblowski, P. Knyphausen, S. de Boor, J. Brenig, A.Y. Zienert, K. Meyer-Teschendorf, G.J. Praefcke, H. Nolte, M. Kruger, M. Schacherl, U. Baumann, L.C. James, J.W. Chin, and M. Lammers. 2016. Structural and Mechanistic Insights into the Regulation of the Fundamental Rho Regulator RhoGDIalpha by Lysine Acetylation. *J Biol Chem*. 291:5484-5499.
- Lam, B.D., and P.L. Hordijk. 2013. The Rac1 hypervariable region in targeting and signaling: a tail of many stories. *Small GTPases*. 4:78-89.
- Lanning, C.C., J.L. Daddona, R. Ruiz-Velasco, S.H. Shafer, and C.L. Williams. 2004. The Rac1 C-terminal polybasic region regulates the nuclear localization and protein degradation of Rac1. *J Biol Chem*. 279:44197-44210.
- Lin, Z., J.Y. Tann, E.T. Goh, C. Kelly, K.B. Lim, J.F. Gao, and C.F. Ibanez. 2015. Structural basis of death domain signaling in the p75 neurotrophin receptor. *Elife*. 4:e11692.
- Liu, M., A.K. Sjogren, C. Karlsson, M.X. Ibrahim, K.M. Andersson, F.J. Olofsson, A.M. Wahlstrom, M. Dalin, H. Yu, Z. Chen, S.H. Yang, S.G. Young, and M.O. Bergo. 2010. Targeting the protein prenyltransferases efficiently reduces tumor development in mice with K-RAS-induced lung cancer. *Proc Natl Acad Sci U S A*. 107:6471-6476.

- Longenecker, K., P. Read, U. Derewenda, Z. Dauter, X. Liu, S. Garrard, L. Walker, A.V. Somlyo, R.K. Nakamoto, A.P. Somlyo, and Z.S. Derewenda. 1999. How RhoGDI binds Rho. *Acta Crystallographica Section D Biological Crystallography*. 55:1503-1515.
- Lu, Y., X. Liu, J. Zhou, A. Huang, J. Zhou, and C. He. 2013. TROY interacts with Rho guanine nucleotide dissociation inhibitor alpha (RhoGDIalpha) to mediate Nogo-induced inhibition of neurite outgrowth. *J Biol Chem*. 288:34276-34286.
- McMahon, H.T., and E. Boucrot. 2015. Membrane curvature at a glance. *J Cell Sci*. 128:1065-1070.
- Michaelson, D., J. Silletti, G. Murphy, P. D'Eustachio, M. Rush, and M.R. Philips. 2001. Differential Localization of Rho Gtpases in Live Cells. *The Journal of Cell Biology*. 152:111-126.
- Moissoglu, K., B.M. Slepchenko, N. Meller, A.F. Horwitz, and M.A. Schwartz. 2006. In vivo dynamics of Rac-membrane interactions. *Mol Biol Cell*. 17:2770-2779.
- Moon, S. 2003. Rho GTPase-activating proteins in cell regulation. *Trends in Cell Biology*. 13:13-22.
- Nalbant, P., L. Hodgson, V. Kraynov, A. Toutchkine, and K.M. Hahn. 2004. Activation of endogenous Cdc42 visualized in living cells. *Science*. 305:1615-1619.
- Naor, Z., O. Benard, and R. Seger. 2000. Activation of MAPK Cascades by G-protein-coupled Receptors: The Case of Gonadotropin-releasing Hormone Receptor. *Trends in Endocrinology & Metabolism*. 11:91-99.
- Neubig, R.R., and D.P. Siderovski. 2002. Regulators of G-protein signalling as new central nervous system drug targets. *Nat Rev Drug Discov*. 1:187-197.
- Nomanbhoy, T.K., J.W. Erickson, and R.A. Cerione. 1999. Kinetics of Cdc42 membrane extraction by Rho-GDI monitored by real-time fluorescence resonance energy transfer. *Biochemistry*. 38:1744-1750.
- Pereira-Leal, J.B., and M.C. Seabra. 2001. Evolution of the Rab family of small GTP-binding proteins. *J Mol Biol*. 313:889-901.
- Pertz, O., L. Hodgson, R.L. Klemke, and K.M. Hahn. 2006. Spatiotemporal dynamics of RhoA activity in migrating cells. *Nature*. 440:1069-1072.
- Philips, M.R., and A.D. Cox. 2007. Geranylgeranyltransferase I as a target for anti-cancer drugs. *J Clin Invest*. 117:1223-1225.
- Pick, E., Y. Gorzalczany, and S. Engel. 1993. Role of the rac1 p21-GDP-dissociation inhibitor for rho heterodimer in the activation of the superoxide-forming NADPH oxidase of macrophages. *Eur J Biochem*. 217:441-455.
- Rak, A., O. Pylypenko, T. Durek, A. Watzke, S. Kushnir, L. Brunsveld, H. Waldmann, R.S. Goody, and K. Alexandrov. 2003. Structure of Rab GDP-dissociation inhibitor in complex with prenylated YPT1 GTPase. *Science*. 302:646-650.
- Resh, M.D. 2006. Trafficking and signaling by fatty-acylated and prenylated proteins. *Nat Chem Biol*. 2:584-590.
- Robbe, K., A. Otto-Bruc, P. Chardin, and B. Antonny. 2003. Dissociation of GDP dissociation inhibitor and membrane translocation are required for efficient activation of Rac by the Dbl homology-pleckstrin homology region of Tiam. *J Biol Chem*. 278:4756-4762.
- Roberts, P.J., N. Mitin, P.J. Keller, E.J. Chenette, J.P. Madigan, R.O. Currin, A.D. Cox, O. Wilson, P. Kirschmeier, and C.J. Der. 2008. Rho Family GTPase modification and dependence on CAAX motif-signaled posttranslational modification. *J Biol Chem*. 283:25150-25163.
- Rolli-Derkinderen, M., V. Sauzeau, L. Boyer, E. Lemichez, C. Baron, D. Henrion, G. Loirand, and P. Pacaud. 2005. Phosphorylation of serine 188 protects RhoA from ubiquitin/proteasome-mediated degradation in vascular smooth muscle cells. *Circ Res*. 96:1152-1160.
- Rossmann, K.L., C.J. Der, and J. Sondek. 2005. GEF means go: turning on RHO GTPases with guanine nucleotide-exchange factors. *Nat Rev Mol Cell Biol*. 6:167-180.

- Sah, V.P., T.M. Seasholtz, S.A. Sagi, and J.H. Brown. 2000. The role of Rho in G protein-coupled receptor signal transduction. *Annu Rev Pharmacol Toxicol.* 40:459-489.
- Scheffzek, K., I. Stephan, O.N. Jensen, D. Illenberger, and P. Gierschik. 2000. The Rac-RhoGDI complex and the structural basis for the regulation of Rho proteins by RhoGDI. *Nat Struct Biol.* 7:122-126.
- Schmidt, A., T. Schmelzle, and M.N. Hall. 2002. The RHO1-GAPs SAC7, BEM2 and BAG7 control distinct RHO1 functions in *Saccharomyces cerevisiae*. *Molecular Microbiology.* 45:1433-1441.
- Schwartz, M. 2004. Rho signalling at a glance. *J Cell Sci.* 117:5457-5458.
- Smith, G.R., S.A. Givan, P. Cullen, and G.F. Sprague Jr. 2002. GTPase-Activating Proteins for Cdc42. *Eukaryotic Cell.* 1:469-480.
- Takahashi, K., T. Sasaki, A. Mammoto, K. Takaishi, T. Kameyama, S. Tsukita, S. Tsukita, and Y. Takai. 1997. Direct Interaction of the Rho GDP Dissociation Inhibitor with Ezrin/Radixin/Moesin Initiates the Activation of the Rho Small G Protein. *Journal of Biological Chemistry.* 272:23371-23375.
- Tcherkezian, J., and N. Lamarche-Vane. 2007. Current knowledge of the large RhoGAP family of proteins. *Biol Cell.* 99:67-86.
- Tnimov, Z., D. Abankwa, and K. Alexandrov. 2014. RhoGDI facilitates geranylgeranyltransferase-I-mediated RhoA prenylation. *Biochem Biophys Res Commun.* 452:967-973.
- Tnimov, Z., Z. Guo, Y. Gambin, U.T. Nguyen, Y.W. Wu, D. Abankwa, A. Stigter, B.M. Collins, H. Waldmann, R.S. Goody, and K. Alexandrov. 2012. Quantitative analysis of prenylated RhoA interaction with its chaperone, RhoGDI. *J Biol Chem.* 287:26549-26562.
- Ueyama, T., J. Son, T. Kobayashi, T. Hamada, T. Nakamura, H. Sakaguchi, T. Shirafuji, and N. Saito. 2013. Negative charges in the flexible N-terminal domain of Rho GDP-dissociation inhibitors (RhoGDIs) regulate the targeting of the RhoGDI-Rac1 complex to membranes. *J Immunol.* 191:2560-2569.
- Ugolev, Y., Y. Berdichevsky, C. Weinbaum, and E. Pick. 2008. Dissociation of Rac1(GDP).RhoGDI complexes by the cooperative action of anionic liposomes containing phosphatidylinositol 3,4,5-trisphosphate, Rac guanine nucleotide exchange factor, and GTP. *J Biol Chem.* 283:22257-22271.
- van den Bogaart, G., K. Meyenberg, H.J. Risselada, H. Amin, K.I. Willig, B.E. Hubrich, M. Dier, S.W. Hell, H. Grubmuller, U. Diederichsen, and R. Jahn. 2011. Membrane protein sequestering by ionic protein-lipid interactions. *Nature.* 479:552-555.
- van Hennik, P.B., J.P. ten Klooster, J.R. Halstead, C. Voermans, E.C. Anthony, N. Divecha, and P.L. Hordijk. 2003. The C-terminal domain of Rac1 contains two motifs that control targeting and signaling specificity. *J Biol Chem.* 278:39166-39175.
- Varshney, P., V. Yadav, and N. Saini. 2016. Lipid rafts in immune signalling: current progress and future perspective. *Immunology.* 149:13-24.
- Wang, M., and P.J. Casey. 2016. Protein prenylation: unique fats make their mark on biology. *Nat Rev Mol Cell Biol.* 17:110-122.
- Wennerberg, K., and C.J. Der. 2004. Rho-family GTPases: it's not only Rac and Rho (and I like it). *J Cell Sci.* 117:1301-1312.
- Worthylake, D.K., K.L. Rossman, and J. Sondek. 2004. Crystal structure of the DH/PH fragment of Dbp without bound GTPase. *Structure.* 12:1078-1086.
- Wu, X., X. Tu, K.S. Joeng, M.J. Hilton, D.A. Williams, and F. Long. 2008. Rac1 activation controls nuclear localization of beta-catenin during canonical Wnt signaling. *Cell.* 133:340-353.
- Xiao, Y., V.Y. Lin, S. Ke, G.E. Lin, F.T. Lin, and W.C. Lin. 2014. 14-3-3tau promotes breast cancer invasion and metastasis by inhibiting RhoGDIalpha. *Mol Cell Biol.* 34:2635-2649.
- Xie, F., S. Shao, A.U.R. Aziz, B. Zhang, H. Wang, and B. Liu. 2017. Role of Rho-specific guanine nucleotide dissociation inhibitor alpha regulation in cell migration. *Acta Histochem.* 119:183-189.
- Yamashita, T., and M. Tohyama. 2003. The p75 receptor acts as a displacement factor that releases Rho from Rho-GDI. *Nat Neurosci.* 6:461-467.

- Zhang, S.C., L. Gremer, H. Heise, P. Janning, A. Shymanets, I.C. Cirstea, E. Krause, B. Nurnberg, and M.R. Ahmadian. 2014. Liposome reconstitution and modulation of recombinant prenylated human Rac1 by GEFs, GDI1 and Pak1. *PLoS One*. 9:e102425.
- Zhou, Y., J.L. Johnson, R.A. Cerione, and J.W. Erickson. 2013. Prenylation and Membrane Localization of Cdc42 Are Essential for Activation by DOCK7. *Biochemistry*. 52:4354-4363.

Erklärung zur Dissertation

Hiermit versichere ich, dass die vorliegende Dissertation von mir selbstständig und ohne unzulässige fremde Hilfe unter Beachtung der Grundsätze zur Sicherung guter wissenschaftlicher Praxis an der Heinrich-Heine-Universität Düsseldorf verfasst worden ist. Die Dissertation wurde in der vorgelegten oder in ähnlicher Form noch bei keiner anderen Institution eingereicht. Ich habe bisher keine erfolglosen Promotionsversuche unternommen.

Düsseldorf, den

Mohammad Akbarzadeh